Iminosugars as Potential Inhibitors of Glycogenolysis: Structural Insights into the Molecular Basis of Glycogen Phosphorylase Inhibition

Nikos G. Oikonomakos,*[,†,‡] Costas Tiraidis,[†] Demetres D. Leonidas,[†] Spyros E. Zographos,[†] Marit Kristiansen,[§] Claus U. Jessen,[§] Leif Nørskov-Lauritsen,[§] and Loranne Agius[||]

Institute of Organic and Pharmaceutical Chemistry and Institute of Biological Research and Biotechnology, The National Hellenic Research Foundation, 48 Vassileos Constantinou Avenue, Athens 11635, Greece, Novo Nordisk A/S, Novo Nordisk Park, DK-2760, Måløv, Denmark, and School of Clinical Medical Sciences, Division of Diabetes, The Medical School, Newcastle upon Tyne NE2 4HH, United Kingdom

Received April 27, 2006

Iminosugars DAB (**5**), isofagomine (**9**), and several *N*-substituted derivatives have been identified as potent inhibitors of liver glycogen phosphorylase a ($IC_{50} = 0.4-1.2\ \mu M$) and of basal and glucagon-stimulated glycogenolysis ($IC_{50} = 1-3\ \mu M$). The X-ray structures of **5**, **9**, and its *N*-3-phenylpropyl analogue **8** in complex with rabbit muscle glycogen phosphorylase (GPb) shows that iminosugars bind tightly at the catalytic site in the presence of the substrate phosphate and induce conformational changes that characterize the R-state conformation of the enzyme. Charged nitrogen N1 is within hydrogen-bonding distance with the carbonyl oxygen of His377 (**5**) and in ionic contact with the substrate phosphate oxygen (**8** and **9**). Our findings suggest that the inhibitors function as oxocarbenium ion transition-state analogues. The conformational change to the R state provides an explanation for previous findings that **5**, unlike inhibitors that favor the T state, promotes phosphorylation of GPb in hepatocytes with sequential inactivation of glycogen synthase.

Introduction

Development of inhibitors of glycogenolysis with pharmaceutical applications in the treatment of type 2 diabetes is a promising therapeutic strategy.[1,2] Glycogen phosphorylase (GP[a]) catalyzes the first step in glycogen degradation to yield glucose-1-P. In the muscle, glucose-1-P is utilized via glycolysis to generate metabolic energy, whereas in liver glucose 1-P, generated during hormonal stimulation of glycogenolysis, mostly is converted to glucose (via glucose 6-P) to maintain blood glucose homeostasis.[3] GP exists in two interconvertible forms, GPb (the nonphosphorylated form, low activity, low substrate affinity, predominantly T state) and GPa (the phosphorylated form, high activity, high substrate affinity, predominantly R state). Allosteric activators, such as AMP, substrate, and substrate analogues or allosteric inhibitors such as ATP, glucose-6-P, glucose, and glucose analogues can alter the equilibrium between the less-active T state and the active R state or vice versa.[4,5] In response to nervous or hormonal signals, GPb is converted to GPa through the phosphorylase kinase-catalyzed addition of a phosphoryl group to a hydroxyl group of a specific serine at the N-terminus. The reverse reaction of dephosphorylation that inactivates the enzyme is catalyzed by protein phosphatase 1 (PP1), an enzyme that is regulated in response to insulin. The T state is a better substrate than the R state for the inactivating enzyme PP1. The conversion of GPa to GPb relieves the allosteric inhibition that GPa exerts on the PP1 associated with the glycogen targeting protein GL, which dephosphorylates glycogen synthase, leading to enzyme activation and stimulation of glycogen synthesis.[6,7] GPa, but not GPb, is a potent inhibitor of the phosphatase action on glycogen synthase, and it is only when GP has been dephosphorylated that the phosphatase is free to activate glycogen synthase,[7] a key regulatory enzyme in glycogen synthesis. Glucose and glucose 6-P are physiological regulators of hepatic glycogen metabolism that act synergistically in promoting the inactivation of GPa leading to sequential activation[8] of glycogen synthase and both diminished glycogen degradation and enhanced glycogen synthesis.

Efforts toward improving glycaemic control in type 2 diabetes have been directed toward developing inhibitors of GP.[1,2,9−14] Inhibitors of hepatic GP have the potential to be effective therapeutic agents for the treatment of type 2 diabetes, as evidenced by studies showing glucose-lowering effects of these compounds.[14,15] Several regulatory binding sites of GP have been identified and are currently under investigation for the design and synthesis of potent inhibitors of the enzyme.[2,12,13,16−23] More specifically, the catalytic site has been probed with glucose analogue inhibitors, designed on the basis of information derived from the crystal structure of the inactive T-state GPb−α-D-glucose complex.[22,24−37] A common feature of these compounds is that upon binding at the catalytic site, they promote the (less-active) T-state conformation of the enzyme through stabilization of the closed position of the 280s loop (residues 282−287), which blocks access of the substrate glycogen to the catalytic site. On transition from T state to R state, the 280s loop becomes disordered and displaced, thus opening a channel that allows a crucial arginine, Arg569, to enter the catalytic site in place of Asp283 and create the recognition site for the substrate phosphate; that also provides access for glycogen substrate to reach the catalytic site[4,5] and promotes a favorable electrostatic environment for the 5′-phosphate of the essential cofactor pyridoxal-5′-phosphate.[38,39] The disordering/displacement of the 280s loop is associated with changes at the subunit−subunit contacts that give rise to allosteric effects. A further significant conformational change in the nonallosteric active maltodextrin

* To whom correspondence should be addressed. Tel.: +30 210 7273 761. Fax: +30 210 7273 831. E-mail: ngo@eie.gr.

[†] Institute of Organic and Pharmaceutical Chemistry, The National hellenic Research Foundation.

[‡] Institute of Biological Research and Biotechnology, The National Hellenic Research Foundation.

[§] Novo Nordisk A/S.

[||] School of Clinical Medical Sciences.

[a] GP, glycogen phosphorylase; 1,4-α-D-glucan/orthophosphate α-glucosyltransferase (EC 2.4.1.1); PP1, protein phosphatase-1; PLP, pyridoxal 5′-phosphate; glucose, α-D-glucose; Glc-1-P, α-D-glucose 1-phosphate; MalP, maltodextrin phosphorylase; rms deviation, root-mean-square deviation.

10.1021/jm060496g CCC: $33.50
Published on Web 08/23/2006

Scheme 1. Chemical Structures of the Iminosugars **10**, **11**, **12**, **5**, **9**, and **8** (showing the numbering system used), the **13** and **14** Analogues, and the Oxocarbenium Ion (**15**)

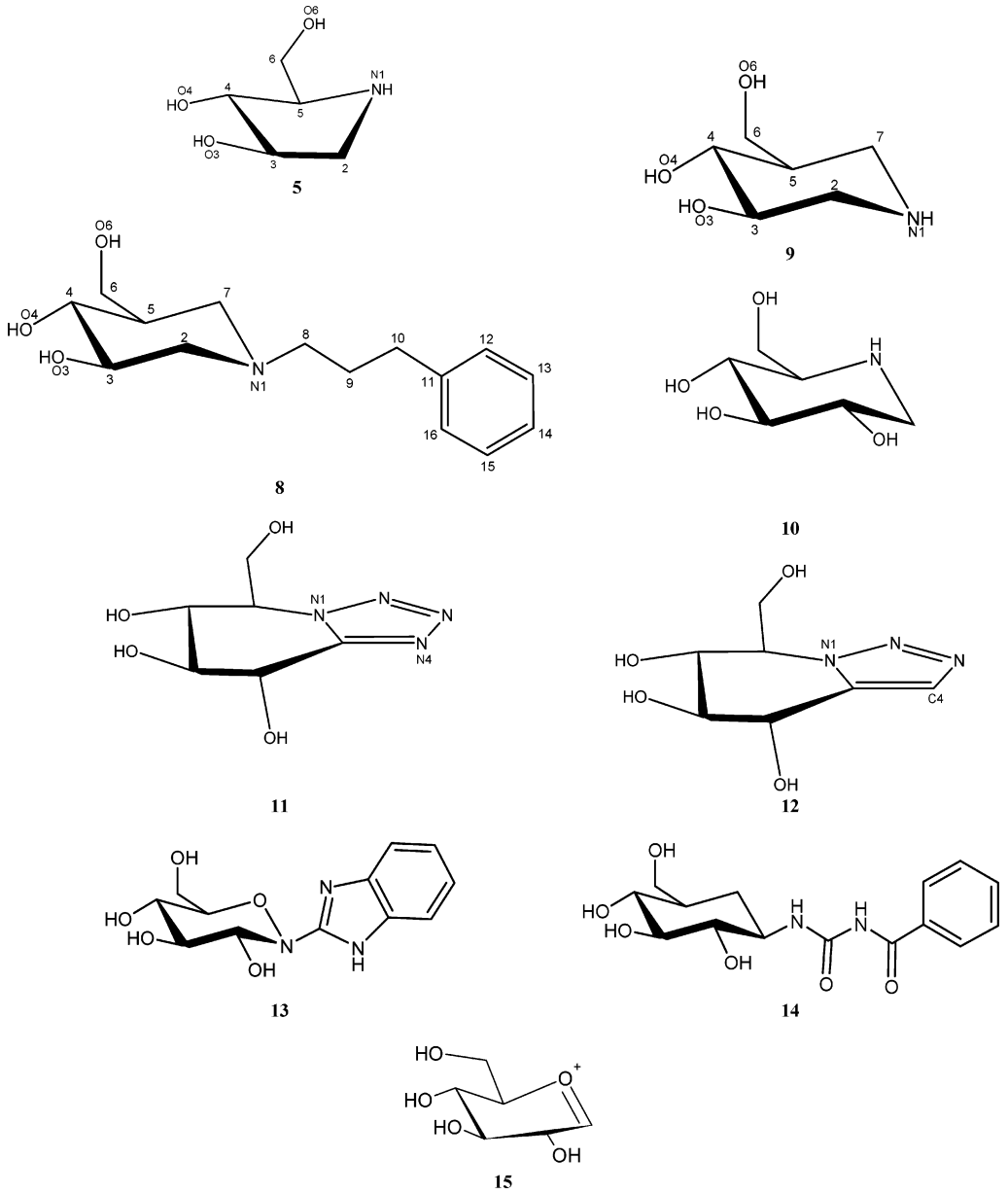

phosphorylase (MalP) structure on binding oligosaccharide (e.g., maltopentaose) involves movement of the 380s loop (residues 377−384), which results in closure of the catalytic site and creation of the recognition site for oligosaccharide.[40]

The phosphorolysis of glycogen catalyzed by GP has been postulated to proceed through a carbenium/oxonium ion transition state (**15**) that is favored and stabilized by the negatively charged phosphate.[40] Therefore, compounds known to mimic the glycosyl cation-like transition state might have the potential to inhibit GP[41] (see Scheme 1). 1-Deoxynojirimycin (**10**), with a nitrogen instead of the ring oxygen, a strong inhibitor of several glycosidases,[42] was found to be a poor inhibitor of GP (K_i = 55 mM).[43] Nojirimycin tetrazole (**11**) has been reported to be a competitive inhibitor of GP with respect to Glc-1-P (K_i = 700 μM) and uncompetitive inihibitor with respect to phosphate (K_i = 53 μM).[44] X-ray crystallographic binding studies to 2.4 Å resolution with GP showed that **11** binds at the catalytic site and promotes the binding of substrate phosphate through ionic contacts with the nitrogen N-1 atom of the tetrazole ring.[44] In contrast, *gluco*-1,2,3-triazole (**12**), where the ring nitrogen N-4 was replaced by CH, exhibited K_i values of 2500 μM (with respect to Glc-1-P) and 540 μM (with respect to phosphate), though the contact between N-1 and the substrate phosphate is maintained in the GP-**12**−phosphate complex.[45] 1,4-Dideoxy-1,4-imino-D-arabinitol (DAB, **5**), a five-membered iminosugar has been identified as a potent inhibitor of muscle and liver glycogen phosphorylase a (GPa).[46,47] In enzyme assays, **5** was shown to be a potent inhibitor of liver GPa (K_i = 0.4 μM), and despite its structural analogy to glucose, it is not synergistic with caffeine. Compound **5** is a potent inhibitor of liver cell glycogenolysis (IC_{50} = 1 μM), it displays antihyperglycaemic effect in obese mice, and it is the most potent inhibitor of basal and glucagon-stimulated glycogenolysis ever reported.[46] In a study of the effects of **5** on the activation state of GP in hepatocytes, it has been demonstrated that **5** promotes phosphorylation rather than dephosphorylation of phosphorylase with concomitant inactivation of glycogen synthase.[10] The six-membered iminosugar NNC 42-1007 (which is identical to isofagomine, **9**) is also a potent inhibitor of liver GPa.[48] Isofagomine was shown to inhibit liver GPa (with an IC_{50} value

Scheme 2

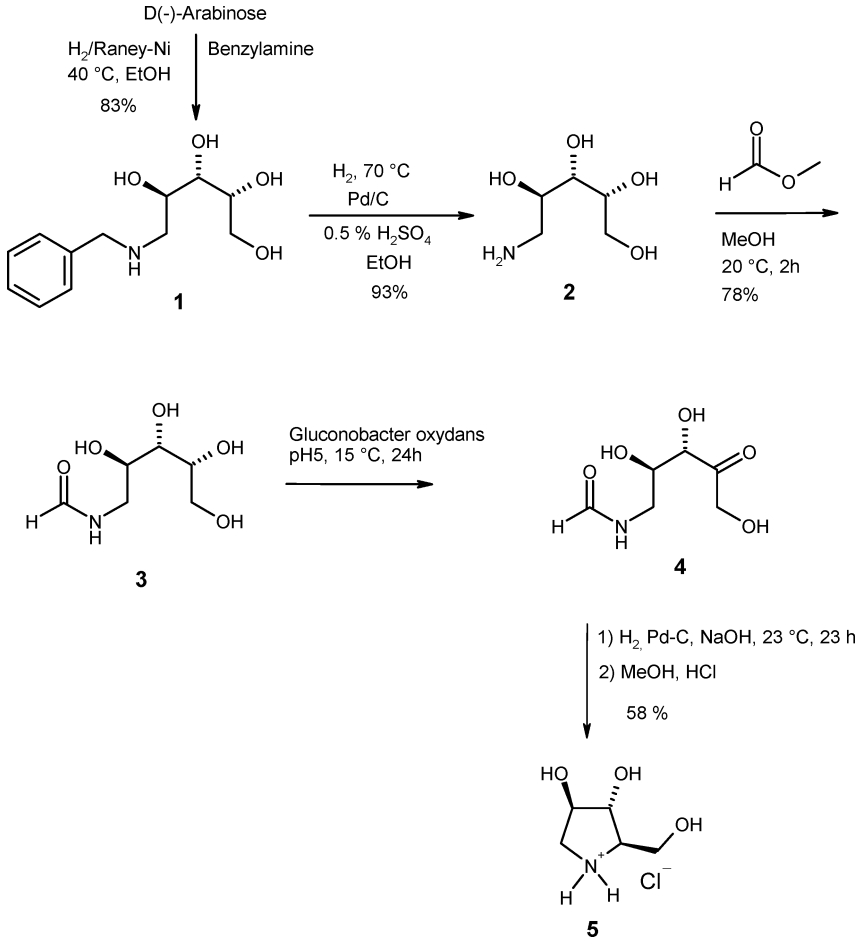

Scheme 3

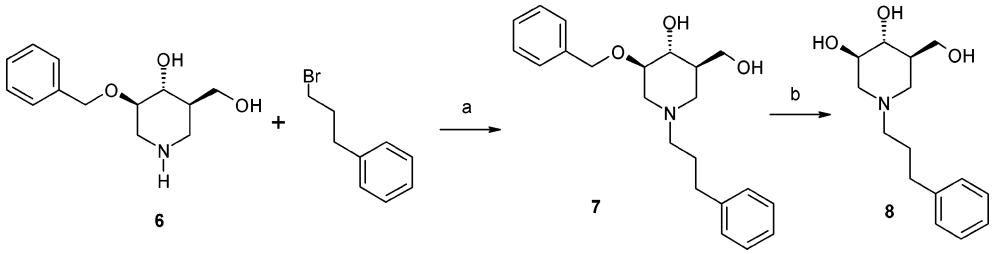

[a] Reagents and conditions: (a) potassium carbonate, KI (cat), dry acetone, 40 °C, 24 h; (b) 96% ethanol, concentrated HCl, 10% Pd/C, H_2, room temperature, 20 h.

of 0.7 μM) and basal and glucagon-stimulated glycogen degradation in cultured hepatocytes (with IC_{50} values of 3.0 and 2.0 μM, respectively).[49] In addition to **9**, several six-membered iminosugars, *N*-substituted and *N*-benzoylmethyl derivatives of **9**, were synthesized and tested for their ability to inhibit GP.[49]

Here we report on the analyses of crystal structures of **5**, **8**, and **9** (Scheme 1) in complex with GPb. The structural results provide detailed insights into the mode of binding of the three iminosugars at the catalytic site, where they occupy a position similar to that of the T-state allosteric inhibitor glucose. Binding of iminosugars, in the presence of phosphate, induces significant conformational changes in the vicinity of the site and promotes the R-state conformation.

Results and Discussion

Chemistry. Compound **5** was synthesized as outlined in Scheme 2 from arabinose in five steps. Reductive amination of D-(−)-arabinose with Raney-Ni and benzylamine in ethanol gave the benzylamino alcohol **1**, which was deprotected with hydrogen in the presence of Pd/C in ethanol to give the primary amine **2**. This amine was protected as the formyl derivative **3**, which was oxidized by gluconobacter oxidans to form **4**. Hydrolysis of the formamide with sodium hydroxide and consecutive reduction of the formed imine gave **5** in an overall yield of 26% in five steps. This new route is a large improvement compared to the published methods, which often involve expensive starting materials and/or several steps. For example, Overkleeft et al.[50] synthesized **5** in seven steps from the expensive 2,3,5-tri-O-benzyl-arabinofuranose, while recently Ayad et al.[51] used 11 steps to synthesize the compound from *cis*-2-butene-1,4-diol.

(3*R*,4*R*,5*R*)-5-Hydroxymethyl-1-(3-phenylpropyl)-3,4-piperidinediol, NNC 42-1326 (**8**),[49] was synthesized as outlined in Scheme 3 by *N*-alkylation of the benzyloxy amine **6** with 3-bromo-1-phenylpropane and subsequent deprotection of the alcohol with hydrogen in the presence of Pd/C in methylene chloride.

Table 1. IC_{50} Values (μM) for Inhibition of the Glycogen Phosphorylase Enzyme

compd	rabbit muscle GPb	rabbit muscle GPa	rat liver GPa	pig liver GPa
5	0.39 ± 0.10	0.33 ± 0.13	0.37 ± 0.09	0.49 ± 0.08
8	0.84 ± 0.13	n.d.[a]	1.22 ± 0.13	0.85 ± 0.18
9	1.21 ± 0.18	0.76 ± 0.04	0.68 ± 0.08	0.67 ± 0.09

[a] n.d. = not determined.

Table 2. Summary of Crystallographic Binding Experiments

	ligand concentration			catalytic site[a]		allosteric site[a]	
exp.	iminosugar	phosphate	soaking time (h)	imino-sugar	phos-phate	phos-phate	resolution (Å)
1	55 mM **5**	55 mM	24	(−)	(−)	(−)	2.26
2	8.8 mM **5**	87 mM	1	(−)	(−)	+	2.26
3	12.4 mM **5**	81 mM	1	(−)	(−)	+	2.26
4	33 mM **5**	400 mM	1	(+)	(+)	+	2.40
5	100 mM **5**	600 mM	1	+	+	+	2.50
6	100 mM **5**	600 mM	15	+	+	+	2.50
7		600 mM	1	(−)	(−)	+	2.26
8	50 mM **9**		3.75	(−)	(−)	(−)	2.10
9	50 mM **9**	400 mM	0.5	+	+	+	2.00
10	10 mM **9**	100 mM	3.75	+	+	+	2.15
11	50 mM **8**		3.75	+	(−)	(−)	2.07
12	65 mM **8**	400 mM	1	+	+	+	2.26
13	10 mM **8**	100 mM	3.75	+	+	+	2.15

[a] The + denotes binding, (+) denotes partial binding, and (−) denotes no binding.

(3*R*,4*R*,5*R*)-5-Hydroxymethyl-3,4-piperidinediol (isofagomine, **9**; Scheme 1) was synthesized as described in the literature.[52]

Enzyme Kinetics. IC_{50} values for inhibition of different isoforms of the GP enzyme for the three compounds, **5**, **8**, and **9**, are shown in Table 1. Compound **5** is generally slightly more potent than the other two compounds, which are nearly equipotent.

X-ray Crystallography. To elucidate the structural basis of inhibition, we have determined the crystal structure of GPb in complex with **5**, **8**, and **9**. A number of experiments were carried out with different ligand concentrations, and a summary of the results is given in Table 2. Not every experiment has presented details (data collection and refinement statistitics). This is because several experiments had negative result and other experiments displayed the same positive result. In the absence of phosphate, neither **5** nor **9** were bound at the catalytic site. In contrast, **8** bound at the catalytic site even in the absence of phosphate. Binding of **5** at the catalytic site showed a dependence on the phosphate concentration. Thus, at 12.4 mM **5** and 81 mM phosphate, there was no binding of either **5** or phosphate at the catalytic site. As the concentrations of both phosphate and **5** were increased, binding was observed at concentrations of phosphate 400 mM or higher. In contrast, binding of isofagomine was observed at lower concentrations of phosphate. Phosphate binding at the catalytic site was accompanied by a disordering or displacement of residues of the 280s loop that resulted in a replacement of the Asp283 by Arg569 (Figure 1). There were no changes at the cap′ (residues 36′−47′), the α2 helix (residues 47−78), and the tower helices α7 (residues 261−274) and α7′ (residues 261′−274′) (where superscript prime refers to residues from the symmetry-related subunit). These regions form the subunit−subunit contacts and are, thus, important for transmission of conformational changes from the subunit−subunit interface to the catalytic site and vice versa. In the absence of iminosugar, there was no binding of phosphate, even at 600 mM, in agreement with previous experiments.[53] In all experiments, with phosphate present, phosphate bound also at the allosteric site. See Supporting Information for crystallographic data collection statistics and refinement for four of the complexes. Portions of the $2F_o-F_c$ electron density maps for ligand molecules bound at the catalytic site are shown in Figure 2. We describe in detail the binary complex GPb−**9** and the obtained ternary complexes GPb−**9**−phosphate, GPb−**8**−phosphate, and GPb−**5**−phosphate.

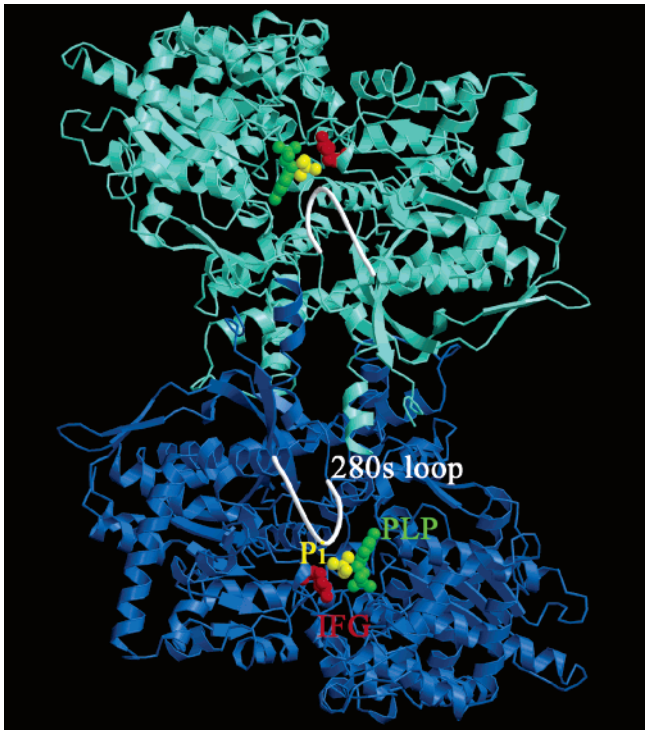

Figure 1. Schematic diagram of the GPb dimeric molecule viewed down the molecular dyad. One subunit is colored in blue and the other in cyan. The position is shown for the catalytic site. The catalytic site, marked by compound **9** (IFG, shown in red), substrate phosphate (Pi, shown in yellow), and the essential cofactor pyridoxal 5′-phosphate (PLP; shown in green), is buried at the center of the subunit and is accessible to the bulk solvent through a 15 Å long channel. Compound **9**, on binding at the catalytic site in the presence of phosphate, promotes the active R state through disordering and displacement of the 280s loop (shown in white). The 280s loop, in the closed position shown here, in the less-active T state, blocks access of the substrate glycogen to the catalytic site.

Binding of 8. The sugar moiety of **8**, on binding at the catalytic site of GP, makes direct specific hydrogen bonds to Glu672 OE1, Ala673 N, Ser674 N, Gly675 N, His377 ND1, and Asn484 through its peripheral hydroxyl groups O3, O4, and O6, and also indirect water-mediated interactions to Thr676 N and OG1 and PLP O3P. The endocyclic nitrogen N1 makes water-mediated contacts to Gly135 N and Asp283 OD1 and OD2 through Wat232 (Figure 3a, and Supporting Information). In fact, the hydrogen bonding network to the peripheral hydroxyls of the sugar moiety is analogous to that observed for the glucopyranose moiety.[24] The 3-phenylpropyl moiety fits neatly into the catalytic site between residues His571, Tyr573, Thr378, Leu380, and Asp283 of the 280s loop, which undergoes conformational changes. Compound **8**, on binding to GPb, makes a total of 9 hydrogen bonds and 60 van der Waals interactions (8 nonpolar/nonpolar, 4 polar/polar, and 48 polar/nonpolar; see Supporting Information).

The superimposition of the structures of the native T-state GPb and the GPb−**8** complex over well-defined residues (24−249, 261−281, 289−313, 326−549, and 558−830) gave rms deviations of 0.168, 0.175, and 0.303 Å for Cα, main-chain,

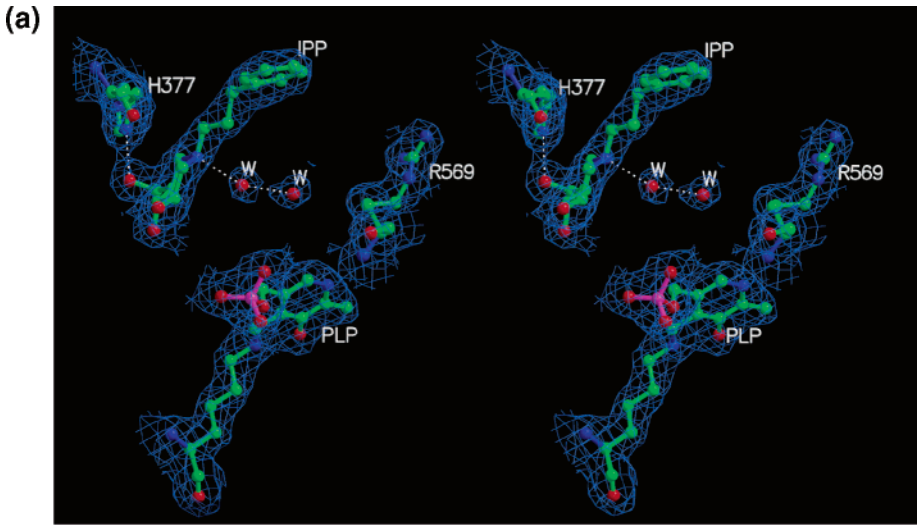
(a)
IPP
H377
W
W
R569
PLP
IPP
H377
W
W
R569
PLP

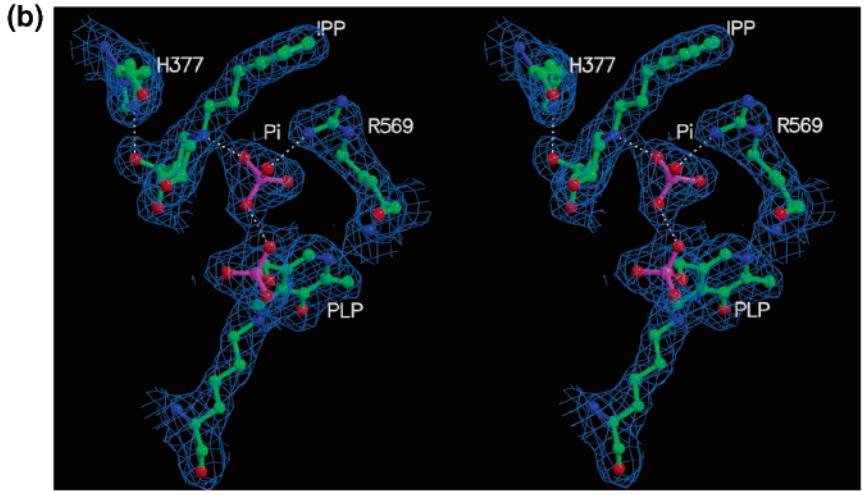
(b)
IPP
H377
Pi
R569
PLP
IPP
H377
Pi
R569
PLP

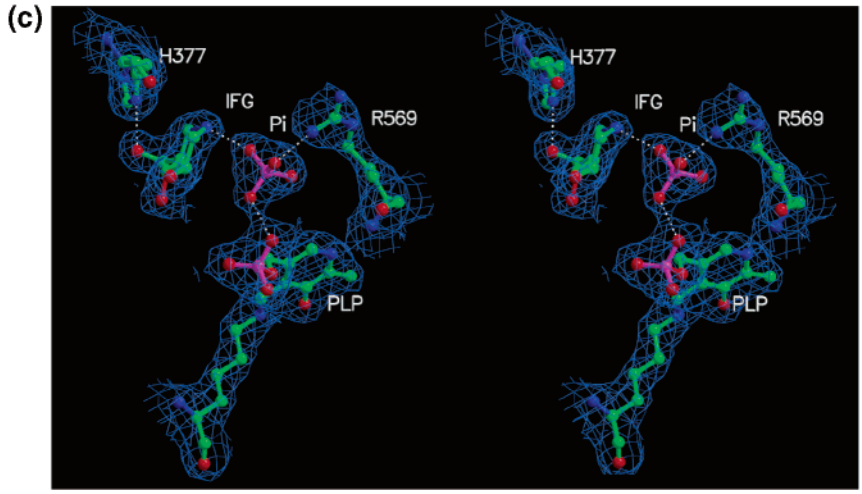
(c)
H377
IFG
Pi
R569
PLP
H377
IFG
Pi
R569
PLP

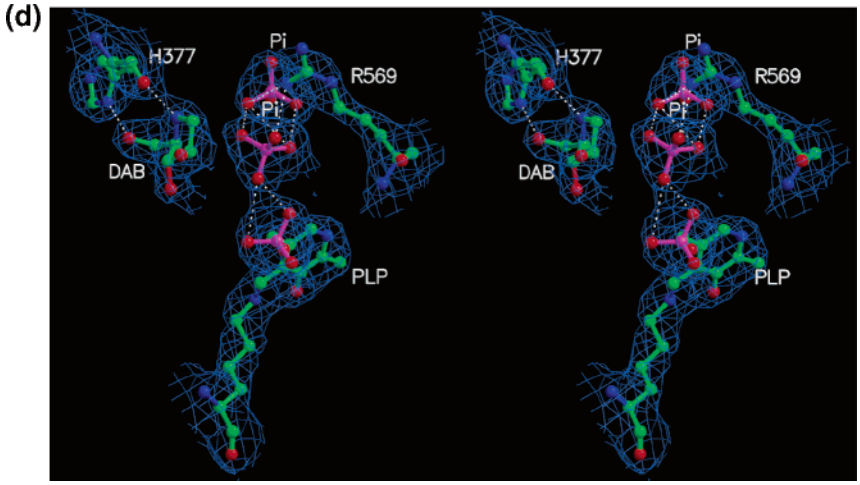

Figure 2. Stereodiagrams of the $2F_o-F_c$ electron density maps, contoured at 1σ, for the bound iminosugars **8** (IPP) in the absence of phosphate (a), **8** (IPP) in the presence of phosphate (b), **9** (IFG) in the presence of phosphate (c), and **5** in the presence of phosphate (d), together with two water molecules (w), PLP (covalently linked to the ϵ-amino group of Lys680, His377, and Arg569 at the catalytic site of GPb. Electron density maps were calculated using the standard protocol, as implemented in REFMAC,[78] before incorporating ligand coordinates.

and side-chain atoms, respectively, indicating that the two structures have very similar conformations. However, there was a major shift in the position of the 280s loop and substantial rearrangements in the side chain of Asn284 (Figure 3b). The shifts for Cα atoms for residues of the 280s loop were 0.4 Å (Pro281), 0.9 Å (Asn282), 1.3 Å (Asp283), 4.2 Å (Asn284), 0.8 Å (Phe285), and 0.3 Å (Phe286) to optimize contacts with the ligand. The greatest changes include shifts of the side-chain atoms of residues Pro281 (0.3−0.5 Å), Asn282 (1.2−1.5 Å), Asp283 (0.8−1.1 Å), Asn284 (6.1−8.7 Å), Phe285 (0.5−0.6 Å), and Phe286 (0.4−0.5 Å). There were also small shifts (0.3−0.6 Å) in Cα atoms for residues of the 380s loop (residues 377−384), the glycine rich helix (residues 133−150), and residues 672−675.

In Figure 3c, we compare the binding of **8** and 2-(β-D-glucopyranosyl)-benzimidazole (**13**) within the catalytic site. Compound **13**[36] is an inhibitor of GPb ($K_i = 8.6 \pm 0.7$ μM) that fits into the "β-pocket", a side channel from the catalytic site, directed toward residue His341 but with no access to the bulk solvent[24] and stabilizes the closed position of the 280s loop in the less-active T-state conformation. In contrast, **8**, on binding to GPb, stabilizes a new conformational motif of the 280s loop at the catalytic site. As a result, the sugar moiety shifts by 0.3−0.8 Å toward residues 672−675. A similar conformational motif of the 280s loop was observed, on *N*-benzoyl-*N*′-β-D-glucopyranosyl urea (**14**) binding, at the catalytic site. Compound **14** binding ($K_i = 4.6$ μM) induces significant shifts for Ca of residues 282−287 (1.0 to 4.1 Å).[32] These conformational changes resulted in increased contacts between the inhibitor and the protein, and the strong affinity of **14** for GPb could be interpreted in terms of its extensive interactions with the protein. A structural comparison between **8** and **14** binding to the catalytic site in the vicinity of the catalytic site is shown in Figure 3d.

Inclusion of phosphate in the GPb−**8**−phosphate complex results in displacement of residues 283−287 of the 280s loop and movement of the side chain of Arg569 to contact phosphate (Figure 3e). Thus, the dihedral angles χ2, χ3, and χ4 of Arg569 change from −66°, −62°, and −106° to 161°, 45°, and −120°, respectively, and the NH1 and NH2 atoms shift by ∼6−7 Å into the catalytic site. Compound **8** binds in an almost identical position whether phosphate is present or not. The interactions that **8** makes with GPb in the ternary complex are similar to those described above, in the binary complex, except that the endocyclic nitrogen N1 interacts with phosphate O2 (2.5 Å). Also, the conformation of phenyl group in the GPb−**8** complex is not identical to that observed in the GPb−**8**−phosphate complex. In the GPb−**8**−phosphate structure, the phenyl group is inclined ∼20° to avoid steric clash with Arg569 NH1 atom. Phosphate binds between the sugar moiety of the ligand and the 5′-phosphate of PLP, with a phosphorus−phosphorus distance of 4.8 Å. The interactions that phosphate makes with GPb are almost identical to those described previously in the GPb−**11**−phosphate[44] and GPb−**12**−phosphate complexes.[45]

Compound **8** is a potent inhibitor of GP with IC_{50} values of 0.84−1.22 μM for various enzyme homologues (Table 1). The potency may result from its extensive interactions with the protein and also from the electrostatic interaction between the assumed protonated N1 ($pK_a = 7.46$; Kristiansen, M., unpublished results) and the substrate phosphate oxygen O2.

Binding of 9. In contrast to **8**, there was no binding of **9** (50 mM) in the absence of phosphate. Detailed kinetic experiments with rabbit muscle GPb showed that **9** is an uncompetitive inhibitor of the enzyme with respect to substrate phosphate (Oikonomakos et al., unpublished results) with a K_i value of 5.2 ± 0.2 μM, a result which is consistent with the crystallographic finding that implies that both **9** and phosphate can bind at the same time. The conformation of the ligand is $^4C_1$, in agreement with the conformation of xylobio−isofagomine as bound to the family 10 xylanase Cex from *Cellulomonas fimi*,[54] and the conformation of isofagomine as bound to sweet almond β-glucosidase[42] but different from the flattened ring conformation observed in the complex of GalNac−isofagomine with *Streptomyces plicatus* β-*N*-acetylhexosaminidase.[55] The mode of the binding of **9** in the presence of the substrate phosphate and the interactions that it makes with the enzyme are almost identical to those described for the sugar moiety of **8** in the ternary complex GPb−**8**−phosphate. There was no electron density for residues Asp283 and Asn284, while residues 282 and 285−287 have increased temperature factors (mean *B* factor of 60 Å^2). The major interaction of **9** with GPb is between the positively charged nitrogen N1 ($pK_a = 8.39$; Kristiansen, M., unpublished results) and phosphate O2. The hydrogen bonding interactions formed between **9** and the protein in the vicinity of the catalytic site are illustrated in Figure 4a, while in Figure 4b, we show a structural comparison between the GPb−**9**−phosphate complex and the GPb−α-D-glucose complex. The positions of the two sugars are similar, with the largest

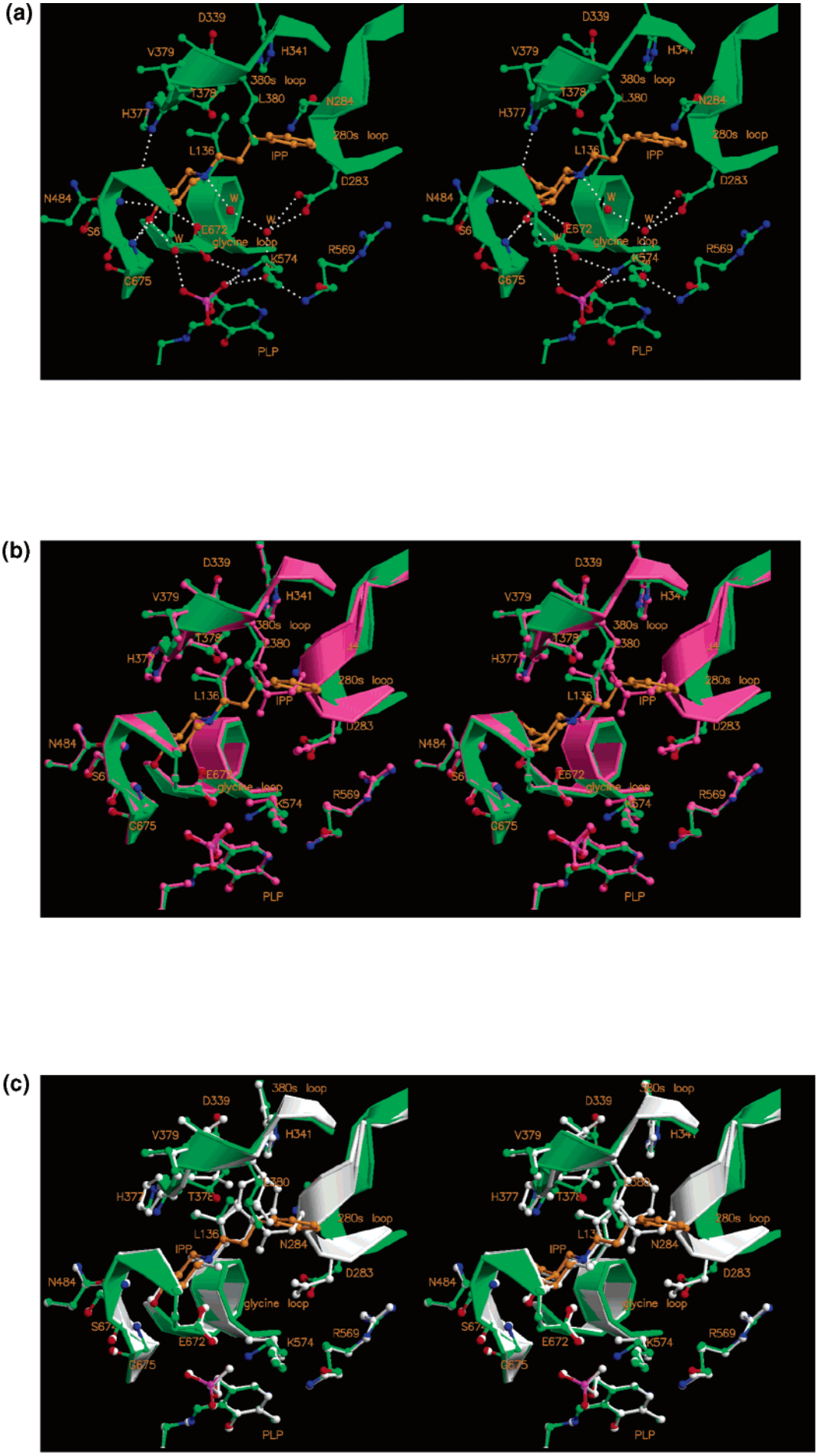
(a)
D339
V379
H341
380s loop
T378
L380
N284
H377
280s loop
L136
IPP
D283
N484
W
S6
E672
glycine loop
R569
K574
G675
PLP
(b)
D339
V379
H341
380s loop
T378
L380
H377
280s loop
L136
IPP
D283
N484
S6
E672
glycine loop
R569
K574
G675
PLP
(c)
380s loop
D339
V379
H341
H377
T378
280s loop
L136
N284
IPP
D283
N484
glycine loop
S67
E672
K574
R569
G675
PLP

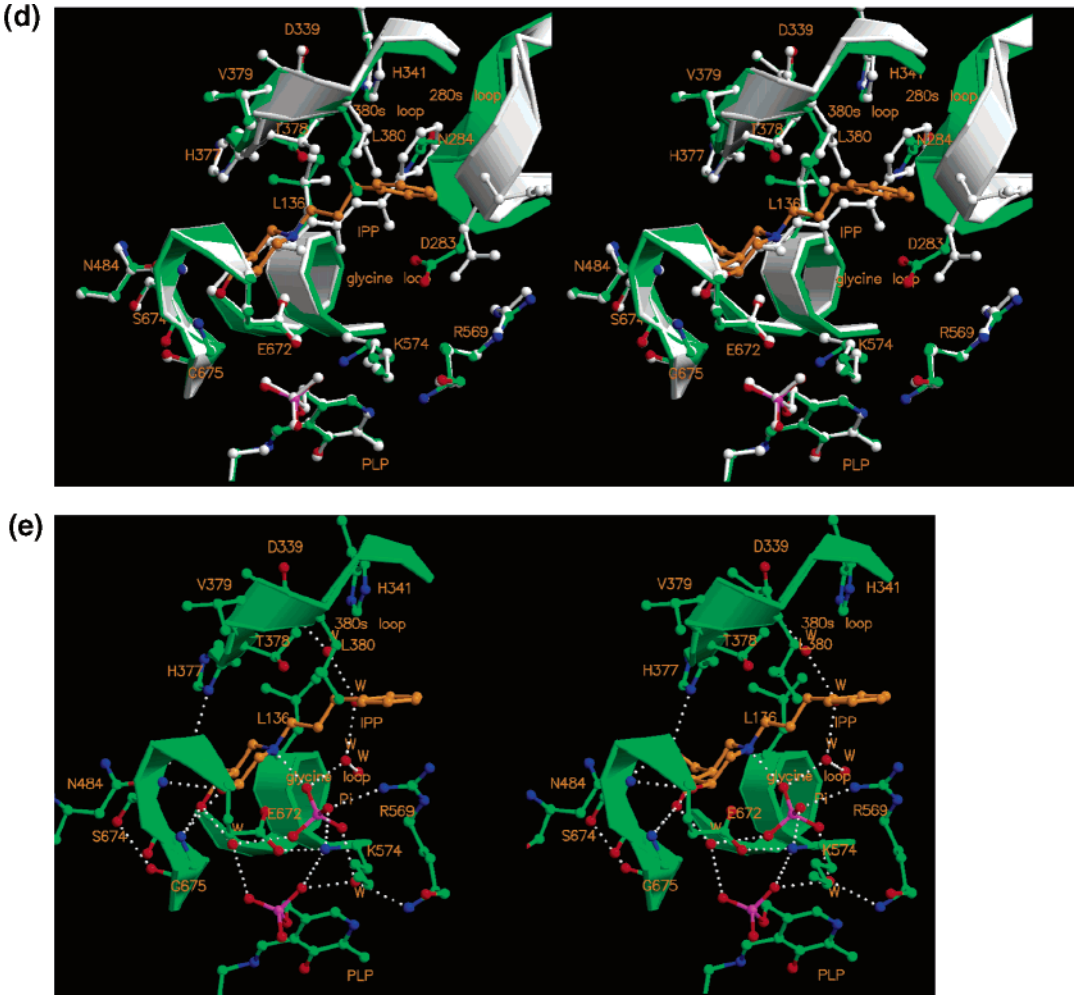

Figure 3. (a) Interactions between **8** (IPP) and protein residues in the vicinity of the catalytic site of GPb. (b) Comparison between GPb−**8** complex (green) and native T state GPb (pink). (c) Comparison between GPb−**8** complex (green) and GPb−**13** complex (white; PDB code 1XKX). (d) Comparison between GPb−**8** complex (green) and GPb−**14** complex (white; PDB code 1K06). (e) Interactions between **8**, phosphate, and protein residues at the catalytic site of GPb. The movement of Arg569 and displacement of the 280s loop are apparent. The hydrogen bond pattern between the inhibitor, protein residues, and water molecules (w) is represented by dotted lines in (a) and (e).

differences in the positions of atoms C7/O5 ∼ 0.5 Å and N1/C1 ∼ 0.6 Å.

Binding of 5. Similarly, **5** (at the concentrations tested) binds to the enzyme only in the presence of a high concentration of phosphate (400−600 mM). However, the conformation of the sugar is ^{N}E, similar to that of the five-membered rings of salacinol and its analogues, as bound to *Drosophila melanogaster* Golgi α-mannosidase II,[56] but differs from the $^{4}C_{1}$ conformation observed for **8** and **9**. As a result, the protonated nitrogen N1 ($pK_a = 8.2$; Kristiansen, M., unpublished results) makes a hydrogen bond to carbonyl O of His377 (2.6 Å), while the distance between phosphate oxygen O2 and N1 is 3.5 Å, rather long for a hydrogen bond. Such a hydrogen bonding interaction between the N1 and the main chain carbonyl oxygen of His377 has not been observed before. This interaction can substantiate the hypothesis that the main chain CO may contribute to the stabilization of the transition-state intermediate.[44] A hydrogen bonding interaction formed between the amide nitrogen of *β*-D-configurated acylamido sugars and the main chain carbonyl O of His377 has been observed in the crystal of T-state GPb complexed with *β*-D-glucopyranosylamine[27,28,33,35,57,58] and spirohydantoin analogues[26,29,31,37,59] of *β*-D-glucopyranose studied so far and also the compound **13**.[36] In contrast, the distance between the protonated N1 and carbonyl O of His377 in the GPb−isofagomine complex is 3.7 Å and in the GPb−**8** complex it is 3.8 Å.

The **5** complex structure showed also the binding of a second phosphate anion in the space occupied by residues Glu88, Leu136, Asp283, and Asn284 in the native structure. The second phosphate anion (PO_4 (2)) is hydrogen bonded to Leu136 N and PO_4 (1) O2 (through O1), to Glu88 OE1 and OE2 (through O2), to Arg569 NH2 (through O3), and to Arg569 NH2 and PO_4 (1) O4 (through O4; see Supporting Information). This second phosphate is distinct from other anionic binding sites that have been observed previously at the catalytic site in both the R and T states.[44,45,60−63] The hydrogen bonding interactions formed between the ligand and the protein are illustrated in Figure 5a.

Energy minimization using the program SYBYL (with the Powell minimizer and the Tripos force field) resulted in a significantly different structure. The computed conformation is $^{4}T_{3}$ (twist). Modeling studies suggest that if **5** in this (twist) conformation were to be incorporated into the enzyme complex, then N1 would interact with both the CO of His377 (∼3 Å) and the phosphate O2 (∼3 Å).

The superimposition of the structures of the native T-state GPb and the GPb−**5**−phosphate complex over well-defined residues (24−249, 261−281, 289−313, 326−549, and 558−830) gave rms deviations of 0.389, 0.394, and 0.686 Å for Cα, main-chain, and side-chain atoms, respectively. The major conformational change on binding of **5** to GPb, in the presence

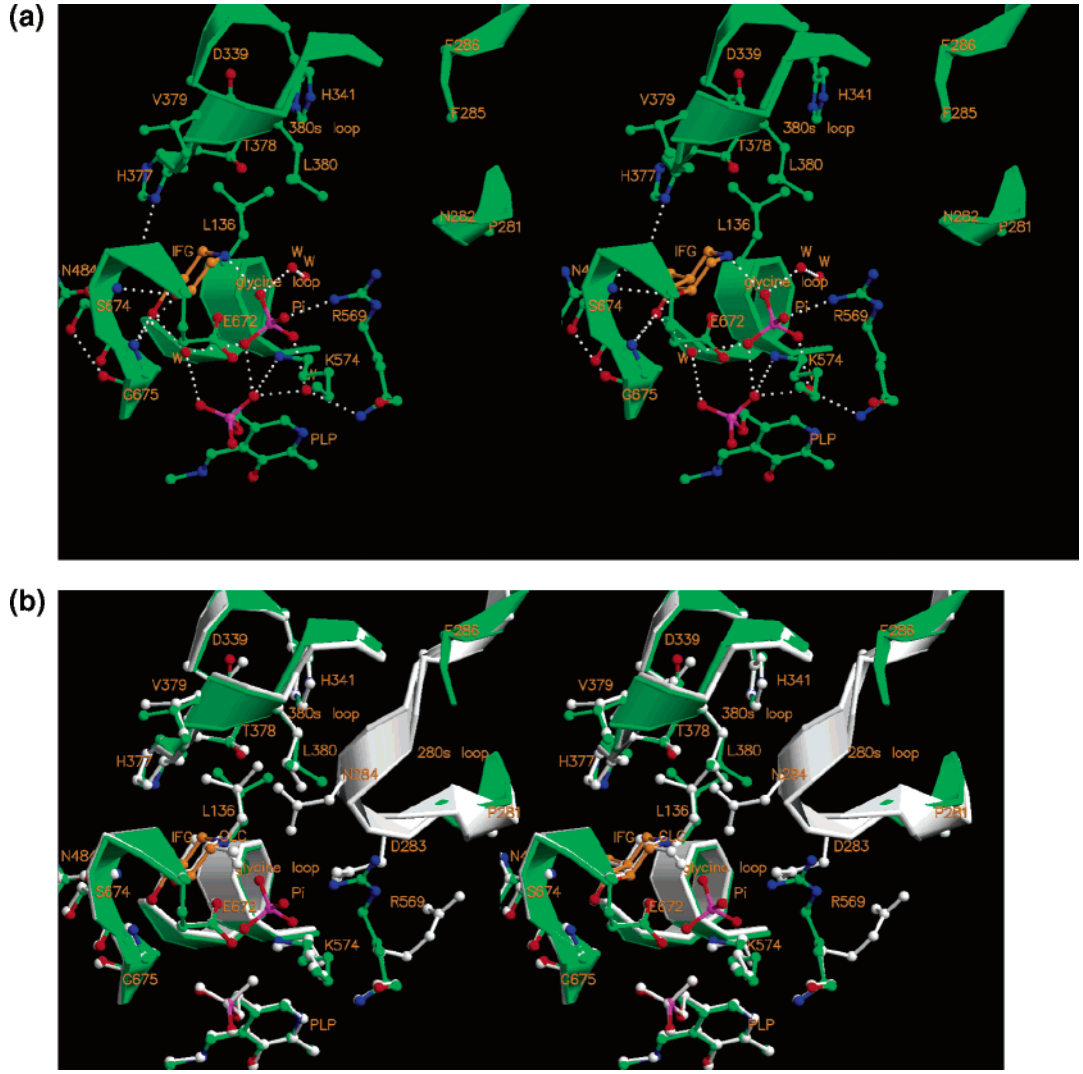

Figure 4. (a) Interactions between **9** (IFG), phosphate, and protein residues in the vicinity of the catalytic site of GPb. (b) Comparison between GPb−**9**−phosphate complex (green) and GPb−α-D-glucose complex (white).

of phosphate, was the replacement of residues 282−285 to create the phosphate recognition site. There were small shifts (between 0.3 and 0.5 Å) in Cα atoms for residues 135−139 and also shifts in Cα atoms (between 0.6 and 1.1 Å) and in side-chain atoms (between 1.0 and 2.0 Å) for residues 377−384, of the 380s loop, toward **5** (Figure 5b). Although the glucosyl recognition pocket at the R-state catalytic site is almost identical to that in the T state, a significant shift was also observed in residues of the 380s loop upon binding of nojirimycin tetrazole to the R-state GPb in the crystal,[44] which contributes to the creation of the glucosyl recognition site.

A comparison of the positions of **5**, **8**, and **9**, phosphate(s), and PLP bound at the catalytic site of the enzyme is shown in Figure 6. It is notable that the positions of the protonated N1 and the carbonyl oxygen of His377, in the GPb−**5**−phosphate complex, differ ∼1.5 Å and 0.8−0.9 Å from their positions in the GPb−**8**−phosphate and GPb−**9**−phosphate complexes, respectively. Also, the substrate phosphate ion in the **5** complex is positioned 0.3−0.4 Å (toward the iminosugar) from the substrate phosphate position in the **8** and **9** complexes.

It has been reported that **5** exhibits uncompetitive (or noncompetitive) inhibition of GPb with respect to the substrate glycogen, at a constant concentrations of AMP (1 mM) and phosphate (45 mM), when the reaction was assayed in the direction of glycogen breakdown, with a K_i value of 342 ± 31 nM (for uncompetitive mode).[47] Similarly, when GPb was assayed with variable concentrations of **5** and phosphate (at a constant AMP concentration of 1 mM and glycogen concentration of 6.17 mM), a K_i value of 396 ± 56 nM was calculated (for uncompetitive mode). These results demonstrate that **5** binds very tightly to the GPb−glycogen−phosphate. Attempts to observe binding of oligosaccharide substrates to the catalytic site of muscle GP in both the T and the R states have not been successful so far. On the contrary, this has been successful with the nonregulatory maltodextrin phosphorylase (MalP). In MalP, the 280s loop is held permanently in an open conformation through interactions with the tower residues, and this creates a constitutively active enzyme that allows access of oligosaccharide substrates to the catalytic site.[40,64−66] The most informative structural results to date have come from a study of the MalP complexed with a good mimic of the substrate maltopentaose, 4-*S*-α-D-glucopyranosyl-4-thio-maltotetraose (GSG4), which is resistant to enzymic cleavage and phosphate.[40]

A structural comparison between the ternary MalP−GSG4−phosphate and GPb−**5**−phosphate complexes in the vicinity of the catalytic site is shown in Figure 7. In the MalP−GSG4−phosphate complex, the oligosaccharide substrate is bound across the catalytic site in subsites −1, +1, and subsequent sites, and the substrate phosphate is within hydrogen bonding distance of the glycosidic oxygen and of the pyridoxal phosphate 5′-

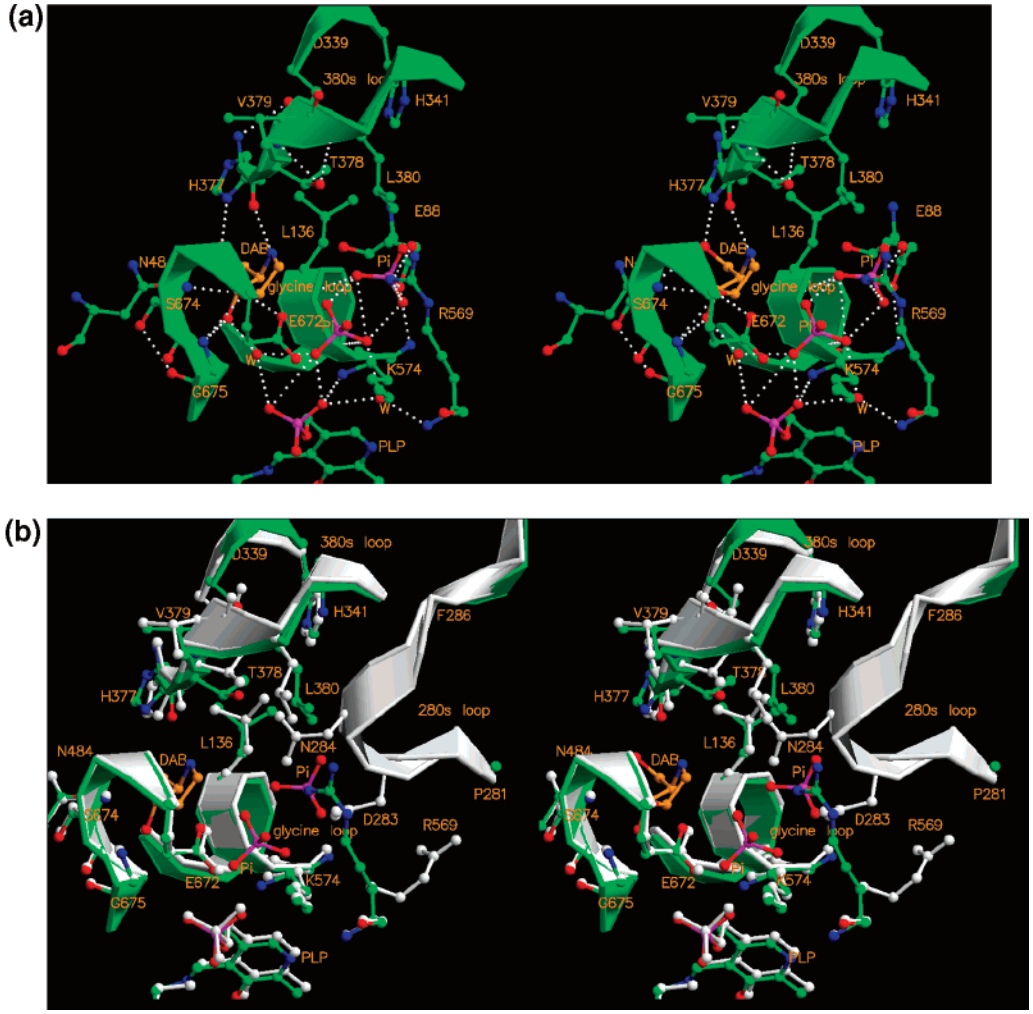

Figure 5. (a) Interactions between **5** (DAB), phosphates, and protein residues at the catalytic site of GPb. (b) Comparison between GPb−**5**−phosphate complex (green) and native T state GPb (white).

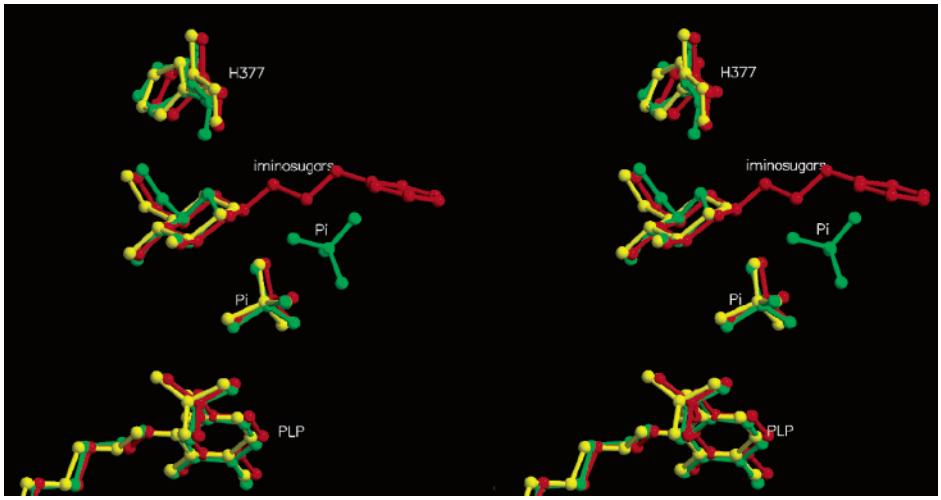

Figure 6. Comparison between GPb−**5**−phosphate (green), GPb−**9**−phosphate (yellow), and GPb−**8**−phosphate (red) complexes, showing the positions of the iminosugars **5**, **8**, **9**, phosphates, PLP, and His377 at the catalytic site of the enzyme.

phosphate group. It has been proposed that the carbonium ion, formed during the first step of the catalytic mechanism for the glycogenolytic reaction, is stabilized by the substrate phosphate, the carbonyl oxygen of His377, and the lone pair electrons on the hydroxyl O3 of the sugar in the subsite +1.[40] In the GPb−**5**−phosphate structure, the position of the substrate phosphate is similar to that observed for the substrate phosphate in the MalP−GSG4−phosphate structure. The N1 of **5** is within 2.5 Å of the "glycosidic" sulfur S4 and 3.3 Å of the hydroxyl O3 of the sugar subsite +1, suggesting that these interactions could contribute to the formation of the GPb−**5**−glycogen−phosphate complex. The corresponding distances of N1 for **9** and **8** complexes are 1.1 and 3.1 Å and 1.2 and 3.2 Å, respectively, suggesting that these iminosugars may disfavor formation and stabilization of the GPb−**9**−glycogen−phosphate and GPb−**8**−glycogen−phosphate complexes.

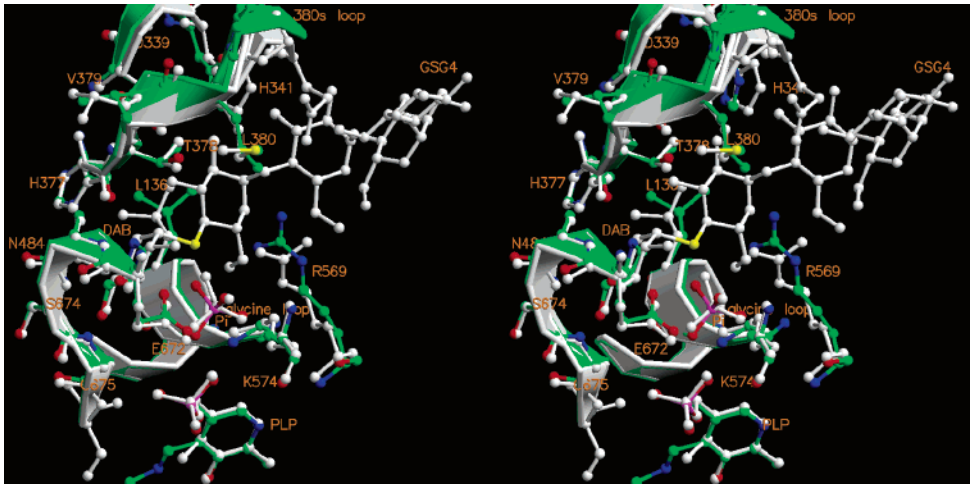

Figure 7. Comparison between GPb−**5**−phosphate complex (green) and MalP−GSG4−phosphate complex (white) in the vicinity of the catalytic site.

On forming the complexes with GPb, in the presence of phosphate, the iminosugar inhibitors become 99.5% (**5**), 94.5% (**8**), and 94.4% (**9**), inaccessible to water, while the corresponding values for ligand and protein buried areas in the GPb−**5**−phosphate, GPb−**9**−phosphate, and GPb−**8**−phosphate ternary complexes are 364.3 Å^2, 366.0 Å^2, and 671.0 Å^2, respectively.

Conclusions

The X-ray crystallographic study of four GPb complexes with iminosugar inhibitors showed that, in the presence of phosphate, compounds **8** and **9** bind tightly at the catalytic site of the enzyme; **5** binds only in the presence of high concentrations of phosphate. The compounds bind at the catalytic site of GPb, with the three hydroxyl groups mimicking the hydroxymethyl and the hydroxyl groups in the O6, O3, and O4 positions in a glucopyranose moiety. Overall, similar conformational rearrangements were observed on binding of the three compounds to the catalytic site of GPb, and this indicates that binding of iminosugars **5**, **8**, and **9** stabilize similar conformations. The major conformational changes on binding of iminosugars to GPb occur in the vicinity of the catalytic site (displacement of residues of the 280s loop, major shifts of residues of the 380s loop). These conformational changes, which characterize the T-to-R allosteric transition, take place without a change in the quaternary structure, and the transmission of the changes to the subunit−subunit interface appears to be suppressed by the lattice contacts that promote the T state. The formation of stable GPb−iminosugar−phosphate complexes require conformational changes in the vicinity of the catalytic site, particularly in the backbone and side chain of residues 282−287. The ligand-induced conformational changes are characteristic for the R-state conformation. Attempts to cocrystallize the enzyme with the iminosugars in the absence or presence of the substrate phosphate, to validate the above argument, have not yielded crystals.

Compounds **9** and **8** form strong electrostatic interactions with substrate phosphate through their protonated and positively charged endocyclic nitrogen N1, and these interactions provide a rationale for their potency to inhibit glycogen phosphorylase. GPb catalytic mechanism proceeds through an oxocarbenium ion intermediate. Although a good transition state analogue should mimic the proposed oxocarbenium ion (**15**) intermediate of the native reaction by adopting a half-chair conformation, distortion of the **9**, and **8**, toward an oxocarbenium-like half-chair conformation was not observed; indeed, both sugar conformations were $^4C_1$. Compound **5** recognition involves His377 of the 380s loop; it is the first compound with a five-membered ring found to bind at the GPb catalytic site, which normally binds glucopyranosyl analogues. Compound **5**, on binding to GPb, in the presence of substrate phosphate, adopts a ^NE conformation, where N1 interacts with CO of His377. Surprisingly, no strong interaction of the substrate phosphate is made with N1 of **5**. To explain why **5** binds weakly in the crystal, we suggest that, **5**, in the presence of glycogen, can interact directly with the hydroxyl groups O3 and O4 of the polysaccharide substrate (subsite +1) through its protonated N1, in addition to its contacts to His377 and the phosphate O2. The contact between O2 and N1 (distance = 3.5 Å) could represent a short-range Coulombic interaction[67] if the phosphate oxygen was negatively charged. It is, therefore, likely that **5**, on binding to the R state, in the presence of both the phosphate and the polysaccharide substrates, has a higher affinity for the GPb−glycogen−phosphate complex, possibly due to the interaction of **5** endocyclic nitrogen with the sugar of the polysaccharide substrate at the subsite +1, in addition to its interaction with His377, and with substrate phosphate, as seen in the GPb−**8**−phosphate and GPb−**9**−phosphate complexes. Overall, we suggest that iminosugars can stabilize phosphate and glycogen binding and inhibit the enzyme directly by mimicking the proposed oxocarbenium ion transition state of the native reaction.

Exposure of hepatocytes to glycogen phosphorylase inhibitors that favor the *T* conformation such as AMP-site inhibitors[68] or indole carboxamides[9,69] promotes conversion of GPa to GPb because the *T* conformation is a better substrate for dephosphorylation by PP-1.[9,68,70] Because GPa is an allosteric inhibitor of glycogen synthase phosphatase by binding to the C-terminus of the liver glycogen targeting protein GL,[70] depletion of GPa by these compounds leads to sequential activation of glycogen synthase and stimulation of glycogen synthesis.[9,68] Compound **5**, in contrast to indole carboxamide inhibitors, promotes conversion of GPb to GPa in hepatocytes, with consequent inactivation of glycogen synthase and inhibition of glycogen synthesis.[10] The present evidence from the crystallography that iminosugars cause the T-to-R transition provides the explanation for the metabolic studies in hepatocytes.[10] Together, the crystallography and physiological experiments on hepatocytes of phosphorylase inhibitors that cause either T-to-R (present study) or R-to-T transition[68,69,71−74] has provided unequivocal support for the physiological role of the regulation of glycogen synthase by the concentration of GPa.

Materials and Methods

Materials. Reagents and solvents were obtained from commercial suppliers and used without further purification. Solvents used were either AR or HPLC grade.

General chemistry. Melting points (uncorrected) were measured on a Büchi-B545 apparatus. ^{1}H and ^{13}C NMR spectra were recorded on a Bruker Advance DPX 200 MHz instrument unless otherwise noted. Chemical shifts are given in ppm (δ) relative to TMS, and coupling constants are in Hz. The HPLC-MS analyses were performed on a PE Sciex API 100 LC/MS system using a Waters 3 mm × 150 mm, 3.5 μm, C-18 symmetry column and a positive ion spray with a flow rate of 20 μL/min. The column was eluted with a linear gradient 10−100% A, in 7.5 min at a flow rate of 1.5 mL/min (solvent A = acetonitrile, 0.01% TFA). Detection: 210 nm. The elemental composition of the compounds agrees to within ±0.4% of the calculated value. The measurement of the optical rotation was performed on a Perkin-Elmer 241 Polarimeter.

(2*R*,3*S*,4*R*)-5-Benzylaminopentane-1,2,3,4,-tetraol (1). D-Arabinose (113.8 g, 750 mmol) was dissolved in 95% ethanol (825 mL). Raney-Ni (11.40 g), concentrated sulfuric acid (0.81 g), and benzylamine (88.60 g, 810 mmol) were added, and the reaction mixture was hydrogenated at 5 bar hydrogen for 20 h at 40−42 °C. The hot reaction mixture was filtered, and the filtrate was slowly cooled to 0 °C, which resulted in precipitation of the product. The precipitate was filtered off, washed with cold water (2 × 45 mL), and dried in vacuo to give **1** as white crystals (yield: 151.0 g (83%)). ^{1}H NMR (DMSO-d_6) in ppm: δ 7.36−7.46 (m, 5H), 4.00 (m, 1H), 3.82 (m, 1H), 3.80 (m, 2H), 3.73 (m, 1H), 3.64 (dd, 1H), 3.48 (m, 1H), 2.80 (dd, 1H), 2.71 (dd, 1H). ^{13}C NMR (DMSO-d_6) in ppm: δ 140.0, 129.5, 129.4, 128.2, 73.0, 72.0, 69.5, 63.8, 53.2, 51.5. LC/MS: *m*/*z* 242 (MH^+). Mp 123.5−124.2 °C (Kagan et al.,[75] mp 122−123 °C).

(2*R*,3*S*,4*R*)-5-Aminopentane-1,2,3,4,-tetraol (2). Pd/C (5%, 4.80 g) and concentrated sulfuric acid (0.22 g, 2.2 mmol) were added to a solution of (2*R*,3*S*,4*R*)-5-benzylaminopentane-1,2,3,4,-tetraol, **1**, (96.4 g, 400 mmol) in 95% ethanol (550 mL). The mixture was hydrogenated at 5 bar hydrogen for 2.5 h at 70−72 °C. The hot reaction mixture was filtered, and the filtrate was concentrated in vacuo to approximately half volume. Upon stirring and cooling to 0 °C, the product precipitated. The product was filtered off, washed with cold water (2 × 30 mL), and dried in vacuo to give **2** as white crystals (yield: 56.4 g (93%)). ^{1}H NMR (DMSO-d_6) in ppm: δ 3.58 (dd, 1H, J = 10.8, J = 3.4 Hz), 3.55 (m, 1H), 3.45 (m, 1H), 3.37 (dd, 1H, J = 10.8, J = 6.0 Hz), 3.27 (dd, 1H, J = 8.0, J = 2.2 Hz), 2.61 (m, 2H). ^{13}C NMR (DMSO-d_6) in ppm: δ 72.4, 71.6, 70.9, 63.6, 45.0. LC/MS: *m*/*z* = 152 (MH^+).

***N*-[(2*R*,3*S*,4*R*)-2,3,4,5-Tetrahydroxypentyl]formamide (3).** Methyl formate (43.6 g, 725 mmol) was added to a solution of 5-aminopentan-1,2,3,4-tetraol, **2**, (50.0 g, 330 mmol) in methanol (1300 mL) at 20 °C. Stirring was continued for 3 h, during which time a white solid precipitated. The mixture was cooled to 0 °C, filtered, and washed with cold methanol (2 × 35 mL) to give **3** (yield: 48.7 g (82%)). ^{1}H NMR (DMSO-d_6) in ppm: δ 8.01 (d, 1H, J = 1.5 Hz), 7.93 (t, 1H, NH, J = 12 Hz), 4.2−4.5 (4H, 4 OH), 3.71 (m, 1H), 3.58 (m, 1H), 3.46 (m, 1H), 3.39 (m, 1H), 3.12−3.20 (m, 2H), 3.08 (m, 1H). ^{13}C NMR (DMSO-d_6) in ppm: δ 161.3, 71.2, 68.4, 63.6, 40.8, 22.5. LC/MS: *m*/*z* = 180 (MH^+).

***N*-[(2*R*,3*S*)-2,3,5-Trihydroxy-4-oxo-pentyl]formamide (4). Biomass Preparation:** Nutrient media (11.5 L; yeast extract (3 g/L), D-sorbitol (60 g/L), soya peptone (5 g/L) in water, pH = 6.3 ± 0.3 with sodium hydroxide) was autoclaved in a 30 L fermentor for 30 min at 121 °C (1 bar), inoculated with *Gluconobacter oxidans* ssp. suboxidans (DSM 2003, 200 mL preculture, same media), and incubated at 30 °C and 200 rpm for 24 h. The fermentation was performed for 13 h at 28 °C at pH 6.3, keeping the amount of oxygen in the fermentation broth above 70% ($P_{O_2}/P_{O_{2(sat)}}$ at atmospheric pressure) by gassing with air. The fermentation broth was cooled to approximately 4 °C. The cells were washed by ultrafiltration with aqueous $MgSO_4$ (20 mM) and concentrated. The concentrated cell suspension was diluted with aqueous $MgSO_4$ (20 mM) to OD_{650nm} 200 and stored at 4 °C.

Bio-Oxidation: Compound **3** (20 g, 111 mmol) was dissolved in deionized water (100 mL). Concentrated cell suspension of *Gluconobacter oxidans* ssp. suboxidans prepared as described above was added, and the pH was adjusted to 5.0 with concentrated hydrochloric acid. The bio-oxidation was performed at 15 °C and pH 5 under shaking. After 24 h, **3** was almost quantitatively converted to raw **4**. The cells were removed by ultrafiltration, and the obtained solution was stored until hydrogenation without further purification.

(2*R*,3*R*,4*R*)-2-Hydroxymethylpyrrolidin-3,4-diol Hydrochloride (5). Pd/C (4%) with 50% water (1.0 g) and 1 M potassium hydroxide (111.9 mL) was added to a solution of raw **4** (100 g, approximately 111 mmol). The mixture was hydrogenated at 5 bar hydrogen for 23 h at room temperature and filtered to give a brownish solution of raw product, which was purified with an ion-exchange resin column (Dowex 50 W × 8 H, 100−200 mesh). The collected fractions were evaporated to dryness in vacuo to give brown oil of (2*R*,3*R*,4*R*)-2-hydroxymethylpyrrolidin-3,4-diol (10.79 g). The oil was dissolved in methanol and $HCl_{(g)}$ was added to give **5** (yield: 11.0 g (58%)). ^{1}H NMR (D_2O) in ppm: δ 4.35 (dt, 1H), 4.11 (t, 1H, J = 6.5 Hz), 3.98 (dd, 1H, J = 4.9, J = 12.4 Hz), 3.85 (dd, 1H, J = 7.8, J = 12.4 Hz), 3.55−3.68 (m, 2H), 3.36 (dd, 1H, J = 2.6, J = 12.4 Hz). ^{13}C NMR (D_2O) in ppm: δ 76.5, 75.2, 68.7, 59.9, 50.9 (NMR-data in agreement with Kagan et al.[75]). Mp 114.8−116.1 °C. $[\alpha]_D$ +35.3 °C (*c* 0.8 in H_2O; Overkleeft et al.,[50] mp 113−115 °C. $[\alpha]_D$ +27.27 °C (*c* 0.47 in D_2O). Purity (>98%) by HPLC. Anal. ($C_5H_{11}NO_3$, HCl) C, H, N.

(3*R*,4*R*,5*R*)-3-Benzyloxy-5-hydroxymethyl-1-(3-phenylpropyl)piperidin-4-ol (7). A mixture of (3*R*,4*R*,5*R*)-3-benzyloxy-5-hydroxymethyl-piperidin-4-ol (**6**, 80 mg, 0.34 mmol), 3-bromo-1-phenylpropane (87 mg, 0.44 mmol), potassium carbonate (140 mg, 1.0 mmol), a pinch of potassium iodide, and dry acetone (8 mL) were stirred at 40 °C for 24 h under a nitrogen atmosphere. The inorganic salts were filtered off, the filtrate evaporated to dryness in vacuo, and the residue purified on a silica gel column (eluent: ethyl acetate/methanol/25% ammonium hydroxide (10/1/1%) to give **7** as an oil (yield: 84 mg (71%)). ^{1}H NMR (CD_3OD) in ppm: δ 7.4−7.1 (m, 10H), 4.70 (q, 2H, J = 11.3 Hz), 3.80 (d, 1H, J = 10.5 Hz), 3.50 (dd, 1H, J = 7.0, 11.2 Hz), 3.35−3.45 (m, 1H), 3.25 (t, 1H, J = 8.7 Hz), 2.93−3.05 (m, 2H), 2.53 (t, 2H, J = 7.5 Hz), 2.33 (m, 2H), 1.75 (m, 5H).

(3*R*,4*R*,5*R*)-5-Hydroxymethyl-1-(3-phenylpropyl)-3,4-piperidinediol Hydrochloride (8). (3*R*,4*R*,5*R*)-3-Benzyloxy-5-hydroxymethyl-1-(3-phenylpropyl)piperidin-4-ol (**7,** 580 mg, 30.2 mmol) was dissolved in 96% ethanol (20 mL). Concentrated hydrochloric acid (0.5 mL) and 10% Pd/C (120 mg) were added, and the mixture was hydrogenated for 20 h at 30 psi. The reaction mixture was filtered and evaporated to dryness in vacuo to give **8** as a golden oil (yield: 0.45 g (92%)). ^{1}H NMR (CD_3OD) in ppm: δ 7.18−7.31 (m, 5H), 3.80 (dd, 1H, J = 3.5, 11.1 Hz), 3.63−3.77 (m, 2H), 3.48−3.62 (m, 2H), 3.36−3.41 (m, 1H), 3.15−3.22 (m, 2H), 2.92 (t, 1H, J = 12.5 Hz), 2.79 (t, 1H, J = 11.6 Hz), 2.71 (t, 2H, J = 7.6 Hz), 2.07−2.15 (m, 2H), 1.93−2.02 (m, 1H). ^{13}C NMR (CD_3OD) in ppm: δ 26.0, 32.5, 41.9, 54.0, 55.5, 57.0, 59.5, 69.3, 71.8, 126.5, 128.5, 128.7, 140.4. Purity (99%) by HPLC.

Enzyme Kinetics. Preparation of pig liver GPa (GPb < 10%) was performed according to literature.[47] Rabbit muscle GPb was obtained from Sigma Chemicals and was activated by 25 μM AMP unless otherwise stated. GP activity was measured in the direction of glycogen breakdown from the photometrical determination of the rate of NADPH formation in an assay coupled to phosphoglucomutase and glucose 6-phosphate dehydrogenase.[47] The enzyme activity was assayed at pH 6.8 and 37 °C in a phosphate buffer containing KH_2PO_4 (18 mM), Na_2HPO_4 (27 mM), $MgCl_2$ (15 mM), EDTA (100 μM), $NADP^+$ (340 μM), glucose 1,6-bisphosphate (4 μM), glucose 6-phosphate dehydrogenase (6000 U/L) and phosphoglucomutase (800 U/L) using a glycogen concentration of 2 mg/mL.

X-ray Crystallography. Native GPb crystals, grown in the tetragonal lattice as described previously from freshly prepared enzyme,[76] spacegroup $P4_32_12$, were soaked with compounds **5**, **8**, and **9** in the absence or presence of phosphate, at concentrations indicated (Table 2), in a buffered solution (10 mM Bes, 0.1 mM EDTA, 0.02% sodium azide, pH 6.7), prior to data collection. Crystallographic data were collected from single crystals on an image plate RAXIS IV using a Rigaku Ru-H3RHB belt drive rotating anode ($\lambda = 1.5418$ Å), operating at 60 kV, 100 mA or an ADSC Q4 CCD detector at EMBL-Hamburg outstation (beamlines $\times$11 and $\times$13) and Daresbury Laboratory (Station 14.2). Crystal orientation, integration of reflections, interframe scaling, partial reflection summation, data reduction, and post-refinement were all performed using DENZO and SCALEPACK.[77]

Crystallographic refinement of the four complexes was performed by maximum-likelihood methods using REFMAC.[78] The starting model employed for the refinement of the complexes was the structure of the native T-state GPb complex determined at 1.9 Å resolution (Oikonomakos et al., unpublished). $2F_o-F_c$ and F_o-F_c electron density maps calculated were visualized using the program for molecular graphics "O".[79] Ligand models, constructed and minimized using the program SYBYL (Tripos Associates, Inc., 1992 SYBYL Molecular Modeling Software, St. Louis, Missouri, U.S.A.), were fitted to the electron density maps after adjustment of their torsion angles. Alternate cycles of manual rebuilding with "O" and refinement with REFMAC improved the quality of the models.

The stereochemistry of the protein residues was validated by PROCHECK.[80,81] Hydrogen bonds and van der Waals interactions were calculated with the program CONTACT, as implemented in CCP4,[81] applying a distance cut off 3.3 and 4.0 Å, respectively. Protein structures were superimposed using LSQKAB.[81] Solvent-accessible areas were calculated with the program NACCESS.[82] All the figures were prepared with the program MolScript[83] and rendered with Raster3D.[84] The coordinates of the new structures have been deposited with the RCSB Protein Data Bank (http://www.rcsb.org/pdb) with the codes 2G9Q (GPb−**8**−phosphate complex), 2G9V (GPb−**9**−phosphate complex), 2G9R (GPb−**8** complex), and 2G9U (GPb−**8**−phosphate complex).

Acknowledgment. This work was supported by the Greek General Secretariat for Research and Technology (GSRT) through the programs PENED-204/2001, Scientific and Technological cooperation between Greece and U.S.A. (2005−2006), Novo Nordisk, the EMBL-Hamburg outstation under FP6 "Structuring the European Research Area Programme", Contract No. RII3/C.T./2004/5060008, and SRS Daresbury Laboratory (Contract IHPP HPRI-CT-1999-00012). The assistance of Dr. V. T. Skamnaki in data collection is also acknowledged.

Supporting Information Available: Crystallographic data collection details for compounds **5**, **8**, and **9**, hydrogen bonding and van der Waals interactions between the inhibitors and GPb residues at the catalytic site, and analytical data for all compounds. This material is available free of charge via the Internet at http://pubs.acs.org.

References

(1) McCormack, J. C.; Westergaard, N.; Kristiansen, M.; Brand, C. L.; Lau, J. Pharmacological approaches to inhibit endogenous glucose production as a means of anti-diabetic therapy. *Curr. Pharm. Des.* **2001**, *7*, 1451−1474.

(2) Treadway, J. L.; Mendys, P.; Hoover, D. J. Glycogen phosphorylase inhibitors for treatment of type 2 diabetes mellitus. *Expert Opin. Invest. Drugs* **2001**, *10*, 439−454.

(3) Newgard, C. B.; Hwang, P. K.; Fletterick, R. J. The family of glycogen phosphorylases: structure and function. *Crit. Rev. Biochem. Mol. Biol.* **1989**, *24*, 69−99.

(4) Johnson, L. N. Glycogen phosphorylase: control by phosphorylation and allosteric effectors. *FASEB J.* **1992**, *6*, 2274−2282.

(5) Oikonomakos, N. G.; Acharya, K. R.; Johnson, L. N. Rabbit muscle glycogen phosphorylase (b) the structural basis of activation and catalysis (review). In *Posttranslational Modification of Proteins*; Harding, J. J., Crabbe, M. J. C, Eds.; CRC Press, Inc.; Boca Raton, Florida, 1992; pp 81−151.

(6) Alemany, S.; Cohen, P. Phosphorylase a is an allosteric inhibitor of the glycogen and microsomal form of rat hepatic protein phosphatase 1. *FEBS Lett.* **1986**, *198*, 194−202.

(7) Bollen, M.; Stalmans, W. The structure, role, and regulation of type 1 protein phosphatase. *Crit. Rev. Biochem. Mol. Biol.* **1992**, *27*, 227−281.

(8) Aiston, S.; Green, A.; Mukhtar, M.; Agius, L. Glucose-6-phosphate causes translocation of phosphorylase in hepatocytes and inactivates the enzyme synergistically with glucose. *Biochem. J.* **2004**, *377*, 195−204.

(9) Aiston, S.; Hampson, L.; Gómez-Foix, A. M.; Guinovart, J. J.; Agius, L. Hepatic glycogen synthesis is highly sensitive to phosphorylase activity. *J. Biol. Chem.* **2001**, *276*, 23858−23866.

(10) Latsis, T.; Andersen, B.; Agius, L. Diverse effects of two allosteric inhibitors on the phosphorylation state of glycogen phosphorylase in hepatocytes. *Biochem. J.* **2002**, *368*, 309−316.

(11) Aiston, S.; Coghlan, M. P.; Agius, L. Inactivation of phosphorylase is a major component of the mechanism by which insulin stimulates hepatic glycogen synthesis. *Eur. J. Biochem.* **2003**, *270*, 2773−2781.

(12) Kristiansen, M.; Andersen, B.; Iversen, L. F.; Westergaard, N. Identification, synthesis, and characterization of new glycogen phosphorylase inhibitors binding to the allosteric AMP site. *J. Med. Chem.* **2004**, *47*, 3537−3545.

(13) Klabunde, T.; Wendt, U. K.; Kadereit, D.; Brachvogel, V.; Burger, H.-J.; Herling, A. W.; Oikonomakos, N. G.; Kosmopoulou, M. N.; Schmoll, D.; Sarubbi, E.; von Roedern, E.; Schönafinger, K.; Defossa, E. Acyl ureas as human liver glycogen phosphorylase inhibitors for the treatment of type 2 diabetes. *J. Med. Chem.* **2005**, *48*, 6178−6193.

(14) Baker, D. J.; Greenhaff, P. L.; Timmons, J. A. Glycogen phosphorylase inhibition as a therapeutic target: a review of the recent patent literature. *Expert Opin. Ther. Pat.* **2006**, *16*, 459−466.

(15) Fosgerau, K.; Mittelman, S. D.; Sunehag, A.; Dea, M. K.; Lundgren, K.; Bergman, R. N. Lack of hepatic "inter-regulation" during inhibition of glycogenolysis in a canine model. *Am. J. Physiol.* **2001**, *281*, E375−E383.

(16) Oikonomakos, N. G. Glycogen phosphorylase as a molecular target for type 2 diabetes therapy. *Curr. Protein Pept. Sci.* **2000**, *3*, 561−586.

(17) Kurukulasuriya, R.; Link, J. T.; Madar, D. J.; Pei, Z.; Richards, S. J.; Rohde, J. J.; Souers, A. J.; Szczepankiewicz, B. G. Potential drug targets and progress towards pharmacologic inhibition of hepatic glucose production. *Curr. Med. Chem.* **2003**, *10*, 123−153.

(18) Lu, Z.; Bohn, J.; Bergeron, R.; Deng, Q.; Ellsworth, K. P.; Geissler, W. M.; Harris, G.; McCann, P. E.; McKeever, B.; Myers, R. W.; Saperstein, R.; Willoughby, C. A.; Yao, J.; Chapman, K. A new class of glycogen phosphorylase inhibitors. *Bioorg. Med. Chem. Lett.* **2003**, *13*, 4125−4128.

(19) Ogawa, A. K.; Willoughby, C. A.; Bergeron, R.; Ellsworth, K. P.; Geissler, W. M.; Myers, R. W.; Yao, J.; Harris, G.; Chapman, K. T. Glucose-lowering in a db/db mouse model by dihydropyridine diacid glycogen phosphorylase inhibitors. *Bioorg. Med. Chem. Lett.* **2003**, *13*, 3405−3408.

(20) Somsák, L.; Nagy, V.; Hadady, Z.; Docsa, T.; Gergely, P. Glucose analogue inhibitors of glycogen phosphorylases as potential antidiabetic agents: recent developments. *Curr. Pharm. Des.* **2003**, *9*, 1177−1189.

(21) Oikonomakos, N. G.; Kosmopoulou, M. N.; Chrysina, E. D.; Leonidas, D. D.; Kostas, I. D.; Wendt, K. U.; Klabunde, T.; Defossa, E. Crystallographic studies on acyl ureas, a new class of glycogen phosphorylase inhibitors, as potential antidiabetic drugs. *Protein Sci.* **2005**, *14*, 1760−1771.

(22) Somsák, L.; Nagy, V.; Hadady, Z.; Felföldi, N.; Docsa, T.; Gergely, P. Recent developments in the synthesis and evaluation of glucose analogue inhibitors of glycogen phosphorylases as potential antidiabetic agents. In *Frontiers in Medicinal Chemistry*; Reitz, A. B., Kordik, C. P., Choudhary, M. I., Atta ur Rahman, Eds; Bentham: Pennington, NJ, 2005; Vol. 2, pp 253−272.

(23) Wright, S. W.; Rath, V. L.; Genereux, P. E.; Hageman, D. L.; Levy, C. B.; McLure, L. D.; McCoid, S. C.; McPherson, R. K.; Schelhorn, T. M.; Wilder, D. E.; Zavadoski, W. J.; Gibbs, E. M.; Treadway, J. L. 5-Chloroindoloyl glycine amide inhibitors of glycogen phosphorylase: synthesis, in vitro, in vivo, and X-ray crystallographic characterization. *Bioorg. Med. Chem. Lett.* **2005**, *15*, 459−465.

(24) Martin, J. L.; Veluraja, K.; Johnson, L. N.; Fleet, G. W. J.; Ramsden, N. G.; Bruce, I.; Orchard, M.; Oikonomakos, N. G.; Papageorgiou, A. C.; Leonidas, D. D.; Tsitura, H. S. Glucose analogue inhibitors of glycogen phosphorylase: the design of potential drugs for diabetes. *Biochemistry* **1991**, *30*, 10101−10116.

(25) Watson, K. A.; Mitchell, E. P.; Johnson, L. N.; Son, J. C.; Bichard, C. J. F.; Orchard, M. G.; Fleet, G. W. J.; Oikonomakos, N. G.; Leonidas, D. D.; Kontou, M.; Papageorgiou, A. C. Design of inhibitors of glycogen phosphorylase: a study of α and *β*-*C*-glucosides and 1-thio-*β*-D-glucose compounds. *Biochemistry* **1994**, *33*, 5745−5758.

(26) Bichard, C. J. F.; Mitchell, E. P.; Wormald, M. R.; Watson, K. A.; Johnson, L. N.; Zographos, S. E.; Koutra, D. D.; Oikonomakos, N. G.; Fleet, G. W. J. Potent inhibition of glycogen phosphorylase by a spirohydantoin of glucopyranose: first pyranose analogues of hydantocidin. *Tetrahedron Lett.* **1995**, *36*, 2145−2148.

(27) Oikonomakos, N. G.; Kontou, M.; Zographos, S. E.; Watson, K. A.; Johnson, L. N.; Bichard, C. J. F.; Fleet, G. W. J.; Acharya, K. R. *N*-acetyl-*β*-D-glucopyranosylamine: a potent T state inhibitor of glycogen phosphorylase. A comparison with α-D-glucose. *Protein Sci.* **1995**, *4*, 2469−2477.

(28) Watson, K. A.; Mitchell, E. P.; Johnson, L. N.; Cruciani, G.; Son, J. C.; Bichard, C. J. F.; Fleet, G. W. J.; Oikonomakos, N. G.; Kontou, M.; Zographos, S. E. Glucose analogue inhibitors of glycogen phosphorylase: from crystallographic analysis to drug prediction using GRID force-field and GOLPE variable selection. *Acta Crystallogr.* **1995**, *D51*, 458−472.

(29) Gregoriou, M.; Noble, M. E. M.; Watson, K. A.; Garman, E. F.; Krülle, T. M.; Fuente, C.; Fleet, G. W. J.; Oikonomakos, N. G.; Johnson, L. N. The structure of a glycogen phosphorylase glucopyranose spirohydantoin complex at 1.8 Å resolution and 100 K: the role of the water structure and its contribution to binding. *Protein Sci.* **1998**, *7*, 915−927.

(30) Somsák, L.; Kovács, L.; Tóth, M.; Õsz, E.; Szilágyi, L.; Györgydeák, Z.; Dinya, Z.; Docsa, T.; Tóth, B.; Gergely, P. Synthesis of and a comparative study on the inhibition of muscle and liver glycogen phosphorylases by epimeric pairs of D-gluco- and D-xylopyranosylidene-spiro-(thio)hydantoins and *N*-(D-glucopyranosyl) amides. *J. Med. Chem.* **2001**, *44*, 2843−2848.

(31) Oikonomakos, N. G.; Skamnaki, V. T.; Õsz, E.; Szilágyi, L.; Somsák L.; Docsa, T.; Tóth, B.; Gergely, P. Kinetic and crystallographic studies of glucopyranosylidene spirothiohydantoin binding to glycogen phosphorylase b. *Bioorg. Med. Chem.* **2002**, *10*, 261−268.

(32) Oikonomakos, N. G.; Kosmopoulou, M.; Zographos, S. E.; Leonidas, D. D.; Chrysina, E. D.; Somsák L.; Nagy, V.; Praly, J.-P.; Docsa, T.; Tóth, B.; Gergely, P. Binding of *N*-acetyl-*N*′-*β*-D-glucopyranosyl urea and *N*-benzoyl-*N*′-*β*-D-glucopyranosyl urea to glycogen phosphorylase b: Kinetic and crystallographic studies. *Eur. J. Biochem.* **2002**, *269*, 1−13.

(33) Chrysina, E. D.; Oikonomakos, N. G.; Zographos, S. E.; Kosmopoulou, M. N.; Bischler, N.; Leonidas, D. D.; Kovács, L.; Docsa, T.; Gergely, P.; Somsák, L. Crystallographic studies on α- and *β*-D-glucopyranosyl formamide analogues, inhibitors of glycogen phosphorylase. *Biocatal. Biotransform.* **2003**, *21*, 233−242.

(34) Györgydeák, Z.; Hadady, Z.; Felföldi, N.; Krakomperger, A.; Nagy, V.; Tóth, M.; Brunyánszki, A.; Docsa, T.; Gergely, P.; Somsák, L. Synthesis of *N*-(beta-D-glucopyranosyl)- and *N*-(2-acetamido-2-deozy-beta-D-glucopyranosyl) amides as inhibitors of glycogen phosphorylase. *Bioorg. Med. Chem.* **2004**, *12*, 4861−4870.

(35) Chrysina, E. D.; Kosmopoulou, M. N.; Kardakaris, R.; Bischler, N.; Leonidas, D. D.; Kannan, T.; Loganathan, T.; Oikonomakos, N. G. Binding of *β*-D-glucopyranosyl bismethoxyphosphoramidate to glycogen phosphorylase (b) kinetic and crystallographic studies. *Bioorg. Med. Chem.* **2005**, *13*, 765−772.

(36) Chrysina, E. D.; Kosmopoulou, M. N.; Tiraidis, C.; Kardakaris, R.; Bischler, N.; Leonidas, D. D.; Hadady, Z.; Somsák, L.; Docsa, T.; Gergely, P.; Oikonomakos, N. G. Kinetic and crystallographic studies on 2-(*β*-D-glucopyranosyl)-5-methyl-1,3,4-oxadiazole, -benzothiazole, and -benzimidazole, inhibitors of muscle glycogen phosphorylase b. Evidence for a new binding site. *Protein Sci.* **2005**, *14*, 873−888.

(37) Watson, K. A.; Chrysina, E. D.; Tsitsanou, K. E.; Zographos, S. E.; Archontis, G.; Fleet, G. W. J.; Oikonomakos, N. G. Kinetic and crystallographic studies of glucopyranose spirohydantoin and glucopyranosylamine analogues inhibitors of glycogen phosphorylase. *Proteins* **2005**, *61*, 966−983.

(38) Johnson, L. N.; Acharya, K. R.; Jordan, M. D.; McLaughlin, P. J. Refined crystal structure of the phosphorylase heptulose-2-phosphate oligosaccharide−AMP complex. *J. Mol. Biol.* **1990**, *211*, 645−661.

(39) Barford, D.; Johnson, L. N. The allosteric transition of glycogen phosphorylase. *Nature (London)* **1989**, *340*, 609−614.

(40) Watson, K. A.; McCleverty, C.; Geremia, S.; Cottaz, S.; Driguez, H.; Johnson, L. N. Phosphorylase recognition and phosphorolysis of its oligosaccharide substrate: answers to a long outstanding question. *EMBO J.* **1999**, *18*, 4619−4632.

(41) Lillelund, V. H.; Jensen, H. H.; Liang, X.; Bols, M. Recent developments of transition-state analogue glycosidase inhibitors of nonnatural product origin. *Chem. Rev.* **2002**, *102*, 515−553.

(42) Zechel, D. L.; Boraston, A. B.; Gloster, T.; Boraston, C. M.; Macdonald, J. M.; Tilbrook, D. M. G.; Stick, R. V.; Davies, G. J. Iminosugar glycosidase inhibitors: structural and thermodynamic dissection of the binding of isofagomine and 1-deoxynojirimycin to *β*-D-glucosidases. *J. Am. Chem. Soc.* **2003**, *125*, 14313−14323.

(43) Ariki, M.; Fukui, T. Affinity of glucose analogues for alpha-glucan phosphorylases from rabbit muscle and potato tubers. *J. Biochem. (Tokyo)* **1977**, *81*, 1017−1024.

(44) Mitchell, E. P.; Withers, S. G.; Ermert, P.; Vasella, A. T.; Garman, E. F.; Oikonomakos, N. G.; Johnson, L. N. Ternary complex crystal structures of glycogen phosphorylase with a transition state analogue nojirimycin tetrazole and phosphate in the T and R states. *Biochemistry* **1996**, *35*, 7341−7355.

(45) Heightman, T. D.; Vasella, A.; Tsitsanou, K. E.; Zographos, S. E.; Skamnaki, V. T.; Oikonomakos, N. G. Cooperative interactions of the catalytic nucleophile and the catalytic acid in the inhibition of *β*-glycosidases. Calculations and their validation by comparative kinetic and structural studies of the inhibition of glycogen phosphorylase b. *Helv. Chem. Acta* **1998**, *81*, 853−864.

(46) Andersen, B.; Rassov, A.; Westergaard, N.; Lundgren, K. Inhibition of glycogenolysis in primary rat hepatocytes by 1,4-dideoxy-1,4-imino-D-arabinitol. *Biochem. J.* **1999**, *342*, 545−550.

(47) Fosgerau, K.; Westergaard, N.; Quistorff, B.; Grunnet, N.; Kristiansen, M.; Lundgren, K. Kinetic and functional characterization of 1,4-dideoxy-1,4-imino-D-arabinitol: a potent inhibitor of glycogen phosphorylase with anti-hyperglycaemic effect in ob/ob mice. *Arch. Biochem. Biophys*. **2000**, *15*, 274−284.

(48) Lundgren, K.; Rassov, A.; Bols, M. NNC 42-1007 is a novel, potent inhibitor of hepatic glycogen phosphorylase, and of hepatocyte glycogenolysis. *Diabetes* **1996**, *45* (Suppl 12), 521.

(49) Jakobsen, P.; Lundbeck, J. M.; Kristiansen, M.; Breinholt, J.; Demuth, H.; Pawlas, J.; Candela, M. P.; Andersen, B.; Westergaard, N.; Lundgren, K.; Asano, N. Iminosugars: Potential inhibitors of liver glycogen phosphorylase. *Bioorg. Med. Chem.* **2001**, *9*, 733−744.

(50) Overkleeft, H. S.; van Wittenburg, J.; Pandit, U. K. A facile transformation of sugar lactones to azasugars. *Tetrahedron* **1994**, *50*, 4215−4224.

(51) Ayad, T.; Génisson, Y.; Broussy, S.; Baltas, M.; Gorrichon, L. A flexible route towards five-membered ring imino sugars and their novel 2-deoxy-2-fluoro analogues. *Eur. J. Org. Chem*. **2003**, *15*, 2903−2910.

(52) Lundgren, K.; Kirk, O. Piperidines and pyrrolidines. WO 95/24391 September 14, 1995.

(53) Hajdu, J.; Acharya, K. R.; Stuart, D. I.; McLaughlin, P. J.; Barford, D.; Oikonomakos, N. G.; Klein, H. W.; Johnson, L. N. Catalysis in the crystal: synchrotron radiation studies with glycogen phosphorylase (b). *EMBO J.* **1987**, *6*, 539−546.

(54) Notenboom, V.; Williams, S. J.; Hoos, R.; Withers, S. G.; Rose, D. R. Detailed structural analysis of glycosidase/inhibitor interactions: complexes of Cex from *Cellulomonas fimi* with xylobiose-derived aza-sugars. *Biochemistry* **2000**, *39*, 11553−11563.

(55) Mark, B. L.; Vocadlo, D. J.; Zhao, D.; Knapp, S.; Withers, S. G.; James, M. N. G. Biochemical and structural assessment of the 1-*N*-aza-sugar galNac-isofagomine as a potent family 20 *β*-*N*-acetylhexosaminidase inhibitor. *J. Biol. Chem.* **2001**, *276*, 42131−42137.

(56) Kuntz, D. A.; Ghavami, A.; Johnston, B. D.; Pinto, B. M.; Rose, D. R. Crystallographic analysis of the interactions of *Drosophila melanogaster* Golgi α-mannosidase II with the naturally occurring glycomimetic salacinol and its analogues. *Tetrahedron: Asymmetry* **2005**, *16*, 25−32.

(57) Anagnostou, E.; Kosmopoulou, M. N.; Chrysina, E. D.; Leonidas, D. D.; Hadjiloi, T.; Tiraidis, C.; Györgydeák, Z.; Somsák, L.; Docsa, T.; Gergely, P.; Oikonomakos, N. G. Crystallographic studies on two bioisosteric analogues, *N*-acetyl-*β*-D-glucopyranosylamine and *N*-trifluoracetyl-*β*-D-glucopyranosylamine, potent inhibitors of muscle glycogen phosphorylase. *Bioorg. Med. Chem.* **2006**, *14*, 181−189.

(58) Hadjiloi, T.; Tiraidis, C.; Chrysina, E. D.; Leonidas, D. D.; Oikonomakos, N. G.; Tsipos, P.; Gimisis, T. Binding of oxalyl derivatives of *β*-D-glucopyranosylamine to muscle glycogen phosphorylase b. *Bioorg. Med. Chem.* **2006**, *14*, 3872−3882.

(59) Somsák, L.; Nagy, V.; Docsa, T.; Tóth, B.; Gergely, P. Gram-scale synthesis of a glucopyranosylidene-spiro-thiohydantoin and its effect on hepatic glycogen metabolism studied in vitro and in vivo. *Tetrahedron: Asymmetry* **2000**, *11*, 405−408.

(60) McLaughlin, P. J.; Stuart, D. I.; Klein, H. W.; Oikonomakos, N. G.; Johnson, L. N. Substrate−cofactor interactions for glycogen phosphorylase b: a binding study in the crystal with heptenitol and heptulose-2-P. *Biochemistry* **1984**, *23*, 5862−5873.
(61) Barford, D.; Hu, S. H.; Johnson, L. N. Structural mechanism for glycogen phosphorylase control by phosphorylation and AMP. *J. Mol. Biol.* **1991**, *218*, 233−260.
(62) Leonidas, D. D.; Oikonomakos, N. G.; Papageorgiou, A. C.; Acharya, K. R.; Barford, D.; Johnson, L. N. Control of phosphorylase b by a modified cofactor: Crystallographic studies on R-state glycogen phosphorylase reconstituted with pyridoxal 5′-diphosphate. *Protein Sci.* **1992**, *1*, 1112−1122.
(63) Sprang, S. R.; Madsen, N. B.; Withers, S. G. Multiple phosphate positions in the catalytic site of glycogen phosphorylase: structure of the pyridoxal-5′-pyrophosphate coenzyme−substrate analogue. *Protein Sci.* **1992**, *1*, 1100−1111.
(64) O'Reilly, M.; Watson, K. A.; Schinzel, R.; Palm, D.; Johnson, L. N. Oligosaccharide substrate binding to *E. coli* maltodextrin phosphorylase. *Nat. Struct. Biol.* **1997**, *4*, 405−412.
(65) O'Reilly, M.; Watson, K. A.; Johnson, L. N. The crystal structure of the *E. coli* maltodextrin phosphorylase-acarbose complex. *Biochemistry* **1999**, *38*, 5337−5345.
(66) Geremia, S.; Campagnolo, M.; Schinzel, R.; Johnson, L. N. Enzymatic catalysis in crystals of *Escherichia coli* maltodextrin phosphorylase. *J. Mol. Biol.* **2002**, *322*, 413−423.
(67) Fisher, B. M.; Schultz, L. W.; Raines, R. T. Coulombic effects of remote subsites on the active site of ribonuclease A. *Biochemistry* **1998**, *37*, 17386−17401.
(68) Bergans, N.; Stalmans, W.; Goldmann, S.; Vanstapel, F. Molecular mode of inhibition of glycogenolysis in rat liver by the dihydropyridine derivative, BAY R3401: inhibition and inactivation of glycogen phosphorylase by an activated metabolite. *Diabetes* **2000**, *49*, 1419−1426.
(69) Martin, W. H.; Hoover, D. J.; Armento, S. J.; Stock, I. A.; McPherson, R. K.; Danley, D. E.; Stevenson, R. W.; Barrett, E. J.; Treadway J. L. Discovery of a human glycogen phosphorylase inhibitor that lowers blood glucose in vivo. *Proc. Natl. Acad. Sci. U.S.A.* **1998**, *95*, 1776−1781.
(70) Bollen, M.; Keppens, S.; Stalmans, W. Specific features of glycogen metabolism. *Biochem. J.* **1998**, *336*, 19−31.
(71) Zographos, S. E.; Oikonomakos, N. G.; Tsitsanou, K. E.; Leonidas, D. D.; Chrysina, E. D.; Skamnaki, V. T.; Bischoff, H.; Goldman, S.; Schram, M.; Watson, K. A.; Johnson, L. N. The structure of glycogen phosphorylase b with an alkyl-dihydropyridine-dicarboxylic acid compound, a novel and potent inhibitor. *Structure* **1997**, *5*, 1413−1425.
(72) Hoover, D. J.; Lefkowitz-Snow, S.; Burgess-Henry, J. L.; Martin, W. H.; Armento, S. J.; Stock, I. A.; McPherson, R. K.; Genereaux, P. E.; Gibbs, E. M.; Treadway, J. L. Indole-2-carboxamide inhibitors of human liver glycogen phosphorylase. *J. Med. Chem.* **1998**, *41*, 2934−2938.
(73) Oikonomakos, N. G.; Skamnaki, V. T.; Tsitsanou, K. E.; Gavalas, N. G.; Johnson L. N. A new allosteric site in glycogen phosphorylase b as a target for drug interactions. *Structure* **2000**, *8*, 575−584.
(74) Rath, V. L.; Ammirati, M.; Danley, D. E.; Ekstrom, J. L.; Gibbs, E. M.; Hynes, T. R.; Mathiowetz, A. M.; McPherson, R. K.; Olson, T. V.; Treadway, J. L.; Hoover, D. J. Human liver glycogen phosphorylase inhibitors bind at a new allosteric site. *Chem. Biol.* **2000**, *7*, 677−682.
(75) Kagan, F.; Rebenstorf, M. A.; Heinzelman, R. V. The preparation of glycamines. *J. Am. Chem. Soc.* **1957**, *79*, 3541−3544.
(76) Oikonomakos, N. G.; Melpidou, A. E.; Johnson, L. N. Crystallization of pig skeletal phosphorylase (b): purification, physical and catalytic characterization. *Biochim. Biophys. Acta* **1985**, *832*, 248−256.
(77) Otwinowski, Z.; Minor, W. Processing of X-ray diffraction data collected in oscillation mode. *Methods Enzymol.* **1997**, *276*, 307−326.
(78) Murshudov, G. N.; Vagin, A. A.; Dodson, E. J. Refinement of macromolecular structures by the Maximum-Likelihood Method. *Acta Crystallogr.* **1997**, *D53*, 240−255.
(79) Jones, T. A.; Zou, J. Y.; Cowan, S. W.; Kjeldgaard, M. Improved methods for the building of protein models in electron density maps and the location of errors in these models. *Acta Crystallogr*. **1991**, *A47*, 110−119.
(80) Laskowski, R. A.; MacArthur, M. W.; Moss, D. S.; Thornton, J. M. PROCHECK − A program to check the stereochemical quality of protein structures. *J. Appl. Crystallogr*. **1993**, *26*, 283−291.
(81) Collaborative Computational Project No 4. The CCP4 suite: Programs for Protein Crystallography. *Acta Crystallogr*. **1994**, *D50*, 760−763.
(82) Hubbard, S. J.; Thornton, J. M. *NACCESS, computer program*, Department of Biochemistry and Molecular Biology, University College London: London, 1993.
(83) Kraulis, P. MOLSCRIPT: a program to produce both detailed and schematic plots of protein structures. *J. Appl. Crystallogr*. **1991**, *24*, 946−950.
(84) Merritt, E. A.; Bacon, D. J. Raster3D: photorealistic molecular graphics. *Methods Enzymol.* **1997**, *277*, 505−524.

JM060496G